TABLE 2. Virus isolation from AFP cases in Cambodia from 1999 to 2003

Identification	No. of cases				
	1999	2000	2001	2002	2003
AFP	149	230	168	155	128
Virus isolated	49	73	46	55	39
Poliovirus[a]	3	9	4	3	4
Nonenterovirus	6	8	4	3	3
HEV-A	3	6	0	9	3
HEV-B	25	26	24	20	13
HEV-C	12	24	15	21	16

[a] OPV-related isolates.

36). The deduced amino acid sequence of the VP1 protein of CAM2033 and CAM2038 showed a high nucleotide identity with those of CAV17 (94.1%) and CAV11-CAV15 (96.7%), respectively. We could not identify the serotype of CAM2083 from the deduced amino acid sequence of the VP1 protein, which showed low similarity with known enteroviruses. We observed the highest amino acid identity only with CAV24 (DN-19 strain) (74.1%) or with a CAV24 variant (73.1%). Consequently, HEV-C isolates in Cambodia in 2002 consisted of CAV1, CAV11-CAV15, CAV17, CAV13-CAV18, CAV20, CAV24, and an untypable HEV-C strain CAM2083 (Table 3).

Sequence analysis of HEV-C isolates in the 3D^{pol} coding region. We then analyzed the genomic sequence in the 3D^{pol} coding region of the HEV-C isolates. The phylogenic analysis of a part of the 3D^{pol} coding region (corresponding to a region of nt 6137 to 6488 of the Sabin 3 genome; 352 nt) showed that the isolates formed distinct genetic clusters from those of the prototype HEV-C strains, as observed for the sequence analysis of the VP4 coding region (Fig. 2). The phylogenic analysis of the 3D^{pol} coding region failed to show a clear relationship between the serotypes of isolates and their genetic clusters. For CAM1974, CAM2083, and CAM2091, we could not obtain the corresponding DNA fragment by RT-PCR. In the phylogenic analysis, a genetic cluster of indigenous CAV13-CAV18 strains was the closest to Cambodia-02. We found that a CAV13-CAV18 isolate (CAM1900) showed the highest nucleotide identity (94.0%) to Cambodia-02 among the HEV-C isolates. We further analyzed the nonstructural protein coding region of CAM1900 and found that CAM1900 showed a high identity to

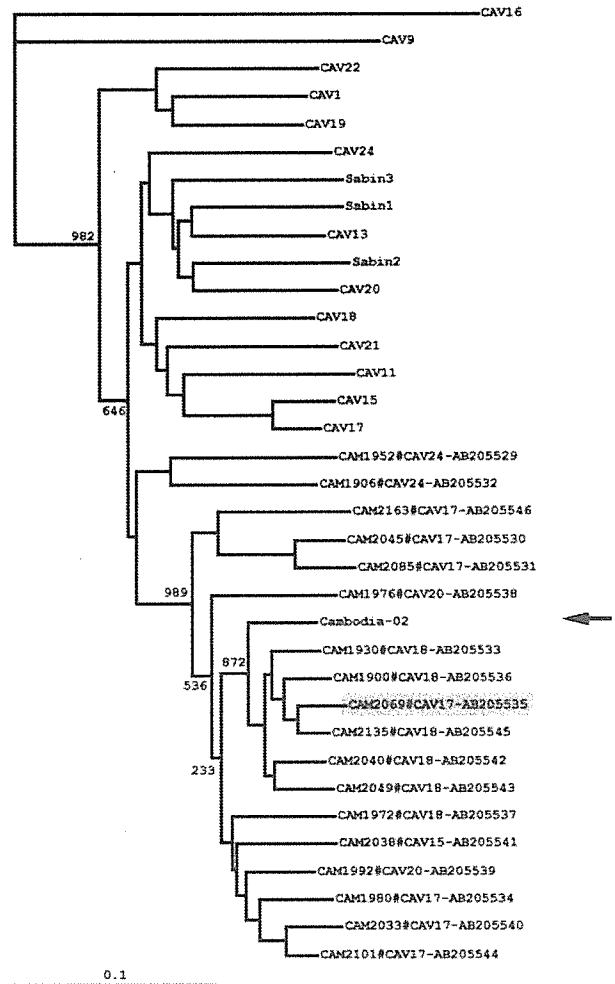

FIG. 2. Phylogenic analysis of the 3D^{pol} coding region. The phylogenic tree was generated from the nucleotide sequences of the 3D^{pol} coding region of Cambodian HEV-C isolates, prototype HEV-C strains, and Sabin strains. The location of Cambodia-02 is indicated by an arrow. A putative HEV-C recombinant (CAM2069) is colored with light gray. The nomenclature of the isolates indicates the names of the isolates, serotypes, and the GenBank/EMBL/DDBJ accession numbers. Bootstrap values are shown at the branch nodes. Bar, 0.1 substitution per site.

TABLE 3. Isolation of HEV-C from AFP cases in Cambodia from 1999 to 2003

HEV-C isolate	No. of isolates				
	1999	2000	2001	2002	2003
CAV1	0	0	0	1	1
CAV11/15	2	3	0	1	3
CAV13/18	2	3	0	7	2
CAV17	1	2	4	7	0
CAV20	2	5	2	2	3
CAV21	0	1	0	0	0
CAV24	2	4	7	2	6
CAM2083	3	6	2	1	1
Total	12	24	15	21	16

Cambodia-02 only in the 3D^{pol} coding region (94.9%) but not in other regions (Fig. 3A and C).

In the phylogenic analysis of the 3D^{pol} coding region, we found that a CAV17 isolate, CAM2069, was located apart from other CAV17 isolates in a genetic cluster of indigenous CAV13-CAV18 strains. The sequence analysis of CAM2069 showed that CAM2069 exhibited a high (95.5 to 97.7%) nucleotide identity to CAM2101 (a CAV17 isolate) for the 2C and the 3AB coding regions. However, the 3CD^{pro} coding region of CAM2069 showed high (93.3 to 95.5%) nucleotide identity to that of CAV13-CAV18, as observed in the phylogenic analysis of the 3D^{pol} coding region (Fig. 2) and in the similarity plot analysis (Fig. 3C). This observation suggested that recombination between CAV13-CAV18 and CAV17 could occur at least in the 3CD^{pro} coding region.

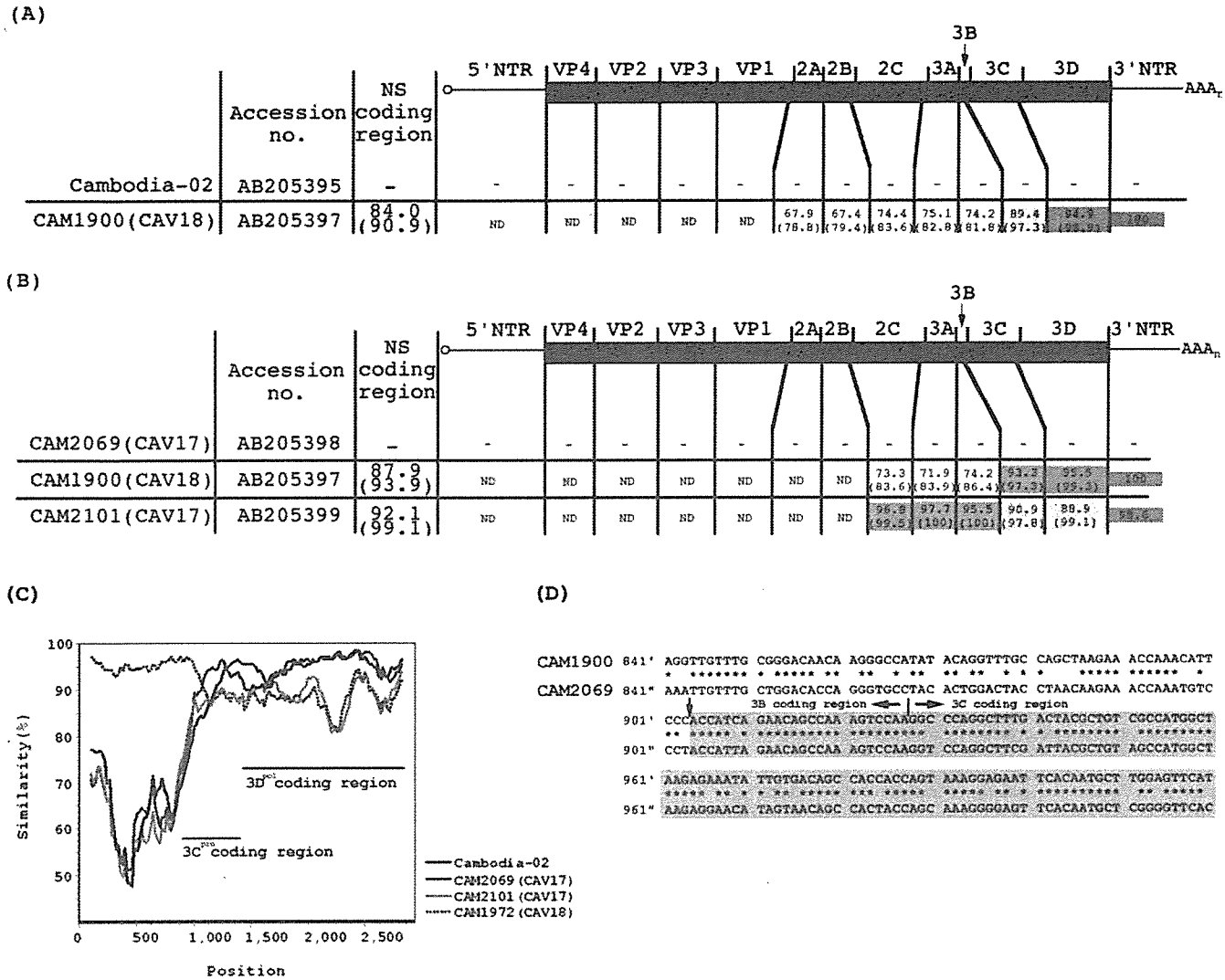

FIG. 3. Alignment of the genomes of Cambodian HEV-C isolates. The numbers in each region represent the percentages of nucleotide identity, and the numbers in parentheses represent the percentages of amino acid identity. The genomic regions that showed more than 90% amino acid identity are colored with light gray, and the genomic regions that showed more than 92% nucleotide identity are colored with dark gray. (A) Alignment of Cambodia-02 with a CAV13-CAV18 isolate (CAM1900). (B) Alignment of a CAV17 isolate (CAM2069) with CAM1900 (CAV13-CAV18) and CAM2101 (CAV17). (C) Multisequence analysis of HEV-C isolates and Cambodia-02 by similarity plot analysis calculated by SimPlot. CAM1900 was used as the reference. A window size of 200 bp with an increment of 20 bp was used. The locations of $3C^{pro}$ and $3D^{pol}$ coding regions are shown in the plot. (D) Alignment of a part of the genome of CAM1900 with that of CAM2069 around the putative recombination junction near the $3C^{pro}$ coding region. The part representing unidentified sequence is colored with gray. NS; nonstructural protein, ND; not determined.

Sequence analysis of HEV-C isolates in the 2BC coding region. Next, we analyzed the sequence of another nonstructural protein coding region of HEV-C isolates, because the analysis in the $3D^{pol}$ coding region failed to identify the recombination counterpart. For this purpose, we designed a new primer set for RT-PCR and DNA sequencing, 2A2+ and 2C−, in the $2A^{pro}$ coding region and in a *cis*-acting replication element in the 2C coding region (19, 40), respectively. By using this primer set, we analyzed a sequence of the 2BC coding region (corresponding to nt 3854 to 4190 of the Sabin 3 genome; 337 nt) for all the NPEV isolates (Fig. 4). We then analyzed the sequence of three isolates (CAM1920, CAM1936, and CAM2034) for which we could not analyze the sequence of the VP4 coding region. However, one isolate (CAM1952, a CAV24 strain) failed to give an RT-PCR product. In the phylogenic analysis of the 2BC coding region, we observed a close relationship between the serotypes of isolates and the genetic clusters. In this phylogenic analysis, Cambodia-02 was again located close to the genetic clusters of indigenous HEV-C but not to those of the HEV-C prototypes. CAM2101 (a CAV17 isolate) showed the highest nucleotide identity to Cambodia-02 in the 2BC coding region; however, the identity was not significantly high (86.9%).

HEV-C isolates from AFP cases in Cambodia from 1999 to 2003. To identify the recombination counterpart of Cambodia-02, we further analyzed the NPEV isolates from 1999 to 2003 in Cambodia. HEV-C was a dominant HEV species isolated from AFP cases in this period, suggesting that the prevalence

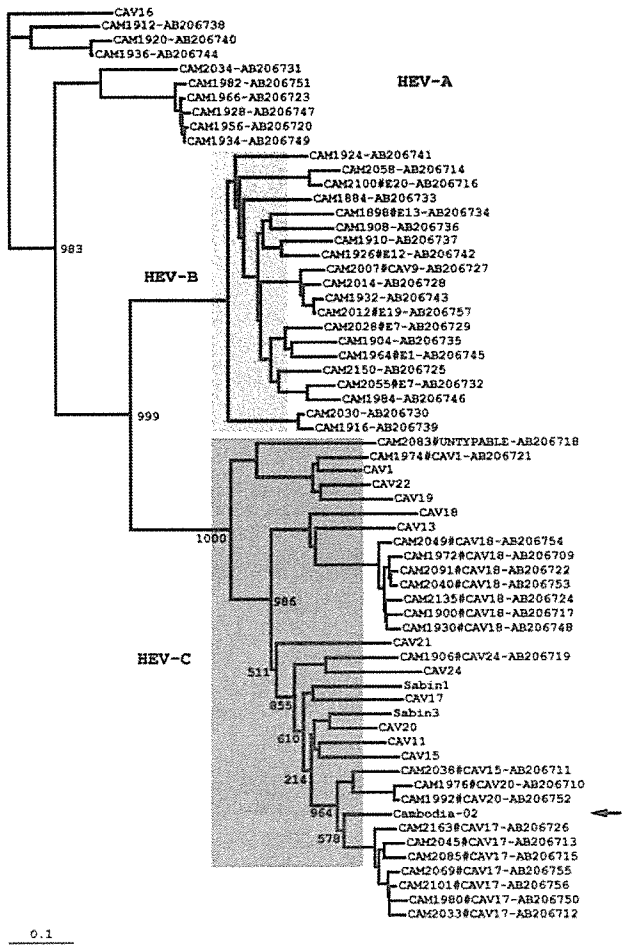

FIG. 4. Phylogenic analysis of the 2BC coding region. The phylogenic tree was generated from the nucleotide sequences in the 2BC coding region of Cambodian NPEV isolates, prototype HEV-C strains, and Sabin strains. The location of Cambodia-02 is indicated by an arrow. The nomenclature of the isolates indicates the names of the isolates, serotypes, and the GenBank/EMBL/DDBJ accession numbers. Bootstrap values are shown at the branch nodes. Bar, 0.1 substitution per site.

of HEV-C was consistently high in Cambodia (Table 2 and 3). The dominant serotypes of HEV-C were different from year to year; in 2002, they were CAV17 and CAV13-CAV18. In the phylogenic analysis of the 2BC coding region, Cambodia-02 was grouped into a cluster of the indigenous CAV15-CAV17-CAV20 isolates. However, the nucleotide identity was not significantly high, and the highest (90.1%) was found with a CAV17 isolate in 2000 (data not shown). Therefore, we could not identify the exact recombination counterpart among the HEV-C isolates examined. However, these results suggested that the recombination counterpart of Cambodia-02 was genetically closely related to the indigenous HEV-C strains in Cambodia.

DISCUSSION

A Sabin 3-derived PV recombinant (Cambodia-02) analyzed in this study was isolated from an AFP case in Cambodia in 2002. Cambodia-02 was classified as OPV-like PV by sequence analysis in the VP1 coding region. In 2002, we isolated three type 3 PVs, including Cambodia-02, from AFP cases in Cambodia, but these PV isolates were genetically unrelated to each other (data not shown). Therefore, this evidence suggested that Cambodia-02 was isolated from a sporadic AFP case and did not result from a circulating strain.

Cambodia-02 was isolated within 6 months after the administration of OPV, as determined on the basis of the previous estimation of the evolution rate of PVs (2, 17). Thus, the unidentified sequence of Cambodia-02 should have retained the original genetic feature of the recombination counterpart. The last indigenous PV case in Cambodia was reported in 1997 (7); therefore, we examined HEV-C strains for the recombination counterpart. We examined HEV-C isolates from AFP cases in Cambodia; however, these isolates represented only a minor population of circulating HEV-C strains that would mostly result in asymptomatic infection. Therefore, through this strategy, we could expect to find some HEV-C strains that were only related to the recombination counterpart. We found that HEV-C was a dominant enterovirus species that could be isolated from the AFP cases in Cambodia (Table 2). The HEV-C isolates consisted of CAV1, CAV11-CAV15, CAV13-CAV18, CAV17, CAV20, CAV21, CAV24, and an untypable serotype represented by CAM2083 (Table 3). HEV-C strains have not been isolated as major NPEVs through the established enterovirus surveillance systems (5, 9) (http://idsc.nih.go.jp/iasr/prompt/circle-g/meningi/menin.html [in Japanese]). However, recently, a high frequency of HEV-C isolation (~50% of the isolates) was reported in Madagascar, where type 2 cVDPVs emerged in 2002 (10, 41). Therefore, HEV-C might be a dominant HEV species among the circulating enteroviruses in tropical areas. However, the prevalence of HEV-C in other tropical areas remained to be further investigated.

We performed a comprehensive sequence analysis of HEV-C isolates in three different genomic regions, including the 2BC coding region and the $3D^{pol}$ coding region (20, 39, 43) (Fig. 2 and 4). We designed a new primer set, 2A2+ and 2C−, for the analysis of the 2BC coding region (Table 1). The 2A2+ primer was designed in the $2A^{pro}$ coding region, and the 2C− primer was designed in a *cis*-acting replication element of the enterovirus (19, 40). This primer set showed a broad spectrum of applicability for HEV-A, HEV-B, and HEV-C isolates, and sequence analysis using this primer set failed for only one isolate (CAM1952 [CAV24]) among 216 NPEV isolates. Recombination junctions of cVDPV have been identified in the 2AB coding region (6, 8, 10, 24). Therefore, with a wide spectrum of applicability for NPEV, this primer set would serve as a useful tool to identify HEV-C strains related to the recombination counterpart of cVDPV.

From the sequence analysis, we found that the nonstructural protein coding regions of Cambodia-02 were grouped into the genetic clusters of the indigenous CAV17 and CAV13-CAV18 strains in Cambodia, distinct from those of the HEV-C prototype strains (Fig. 2 and 4). We isolated CAV17 from 2001 to 2002 and CAV13-CAV18 from 2002 to 2003. Thus, both CAV17 and CAV13-CAV18 were highly prevalent and could be available as the recombination counterpart of Cambodia-02 in 2002. One of the CAV13-CAV18 isolates (CAM1900) showed the highest (94.9%) nucleotide identity to Cambo-

dia-02 in the $3D^{pol}$ coding region (Fig. 4). The nucleotide identities in the $3D^{pol}$ coding region among isolates with the same HEV-C serotype isolated in 2002 were 95 to 96% (Fig. 3), and Cambodia-02 showed a nucleotide identity comparable to indigenous HEV-C isolates in 2002. This suggested that these HEV-C isolates had evolved independently before the putative epidemic in 2002. Interestingly, we found a putative CAV recombinant (CAM2069) in the $3CD^{pro}$ coding region, suggesting frequent interserotypic recombination between CAV17 and CAV13-CAV18 in this region (Fig. 4). Actually, the $3CD^{pro}$ coding region showed high similarities among CAV13-CAV18, CAV11-CAV15, CAV17, and CAV20 (4, 22). This was reminiscent of frequent recombination among HEV-B strains and also among human rhinoviruses where the $3D^{pol}$ coding regions of the same serotype were not monophyletic (27, 30, 38, 47). However, we could not find the exact recombination counterpart among the indigenous HEV-C isolates from AFP cases, although their nonstructural protein coding region was closely related to that of Cambodia-02.

In summary, we isolated a type 3 PV recombinant from an AFP case in Cambodia and suggested that the unidentified sequence of the recombinant was derived from an indigenous HEV-C strain in Cambodia. In addition to the poor population immunity, the high prevalence of HEV-C would be another critical factor for the emergence and/or the evolution of cVDPV. The biological roles of the recombination of cVDPV remain to be further studied.

ACKNOWLEDGMENTS

We thank Keith Feldon and Cambodian local and regional EPI staffs for their expert surveillance. We are grateful to Junko Wada for her excellent assistance.

This work was supported by grants-in-aid for "Promotion of Polio Eradication" from the Ministry of Health, Labor and Welfare, Japan, and by a grant for health research from the regional office for the Western Pacific, World Health Organization. H.S. was supported in part by grants-in-aid for "Development of Expanded Programme on Immunization and Accelerating Measles Control in the Polio-free Era" from the Ministry of Health, Labor and Welfare, Japan.

REFERENCES

1. **Alexander, J. P., Jr., H. E. Gary, Jr., and M. A. Pallansch.** 1997. Duration of poliovirus excretion and its implications for acute flaccid paralysis surveillance: a review of the literature. J. Infect. Dis. **175:**S176–S182.
2. **Bellmunt, A., G. May, R. Zell, P. Pring-Akerblom, W. Verhagen, and A. Heim.** 1999. Evolution of poliovirus type I during 5.5 years of prolonged enteral replication in an immunodeficient patient. Virology **265:**178–184.
3. **Boot, H. J., D. T. Kasteel, A. M. Buisman, and T. G. Kimman.** 2003. Excretion of wild-type and vaccine-derived poliovirus in the feces of poliovirus receptor-transgenic mice. J. Virol. **77:**6541–6545.
4. **Brown, B., M. S. Oberste, K. Maher, and M. A. Pallansch.** 2003. Complete genomic sequencing shows that polioviruses and members of human enterovirus species C are closely related in the noncapsid coding region. J. Virol. **77:**8973–8984.
5. **Caro, V., S. Guillot, F. Delpeyroux, and R. Crainic.** 2001. Molecular strategy for 'serotyping' of human enteroviruses. J. Gen. Virol. **82:**79–91.
6. **Centers for Disease Control and Prevention.** 2001. Acute flaccid paralysis associated with circulating vaccine-derived poliovirus—Philippines, 2001. Morb. Mortal. Wkly. Rep. **50:**874–875.
7. **Centers for Disease Control and Prevention.** 2001. Certification of poliomyelitis eradication—Western Pacific Region, October 2000. Morb. Mortal. Wkly. Rep. **50:**1–3.
8. **Centers for Disease Control and Prevention.** 2001. Circulation of a type 2 vaccine-derived poliovirus—Egypt, 1982–1993. JAMA **285:**1148–1149.
9. **Centers for Disease Control and Prevention.** 2002. Enterovirus surveillance—United States, 2000–2001. Morb. Mortal. Wkly. Rep. **51:**1047–1049.
10. **Centers for Disease Control and Prevention.** 2002. Poliomyelitis—Madagascar, 2002. Morb. Mortal. Wkly. Rep. **51:**622.
11. **Centers for Disease Control and Prevention.** 1997. Progress toward poliomyelitis eradication—Western Pacific Region, January 1, 1996-September 27, 1997. Morb. Mortal. Wkly. Rep. **46:**1113–1117.
12. **Cherkasova, E. A., E. A. Korotkova, M. L. Yakovenko, O. E. Ivanova, T. P. Eremeeva, K. M. Chumakov, and V. I. Agol.** 2002. Long-term circulation of vaccine-derived poliovirus that causes paralytic disease. J. Virol. **76:**6791–6799.
13. **Evans, D. M., G. Dunn, P. D. Minor, G. C. Schild, A. J. Cann, G. Stanway, J. W. Almond, K. Currey, and J. V. Maizel.** 1985. Increased neurovirulence associated with a single nucleotide change in a noncoding region of the Sabin type 3 poliovaccine genome. Nature **314:**548–550.
14. **Felsenstein, J.** 1985. Confidence limits on phylogenies: an approach using the bootstrap. Evolution **39:**783–791.
15. **Filman, D. J., R. Syed, M. Chow, A. J. Macadam, P. D. Minor, and J. M. Hogle.** 1989. Structural factors that control conformational transitions and serotype specificity in type 3 poliovirus. EMBO J. **8:**1567–1579.
16. **Fine, P. E., and I. A. Carneiro.** 1999. Transmissibility and persistence of oral polio vaccine viruses: implications for the global poliomyelitis eradication initiative. Am. J. Epidemiol. **150:**1001–1021.
17. **Gavrilin, G. V., E. A. Cherkasova, G. Y. Lipskaya, O. M. Kew, and V. I. Agol.** 2000. Evolution of circulating wild poliovirus and of vaccine-derived poliovirus in an immunodeficient patient: a unifying model. J. Virol. **74:**7381–7390.
18. **Gelfand, H. M., P. L., D. R. LeBlanc, and J. P. Fox.** 1959. Revised preliminary report on the Louisiana observations of the natural spread within families of living vaccine strains of poliovirus, p. 203–217. First international conference on live poliovirus vaccines. Pan American Sanitary Bureau, Washington, D.C.
19. **Goodfellow, I., Y. Chaudhry, A. Richardson, J. Meredith, J. W. Almond, W. Barclay, and D. J. Evans.** 2000. Identification of a *cis*-acting replication element within the poliovirus coding region. J. Virol. **74:**4590–4600.
20. **Guillot, S., V. Caro, N. Cuervo, E. Korotkova, M. Combiescu, A. Persu, A. Aubert-Combiescu, F. Delpeyroux, and R. Crainic.** 2000. Natural genetic exchanges between vaccine and wild poliovirus strains in humans. J. Virol. **74:**8434–8443.
21. **Horie, H., H. Yoshida, K. Matsuura, M. Miyazawa, Y. Ota, T. Nakayama, Y. Doi, and S. Hashizume.** 2002. Neurovirulence of type 1 polioviruses isolated from sewage in Japan. Appl. Environ. Microbiol. **68:**138–142.
22. **Hyypia, T., T. Hovi, N. J. Knowles, and G. Stanway.** 1997. Classification of enteroviruses based on molecular and biological properties. J. Gen. Virol. **78:**1–11.
23. **Ishiko, H., Y. Shimada, M. Yonaha, O. Hashimoto, A. Hayashi, K. Sakae, and N. Takeda.** 2002. Molecular diagnosis of human enteroviruses by phylogeny-based classification by use of the VP4 sequence. J. Infect. Dis. **185:**744–754.
24. **Kew, O., V. Morris-Glasgow, M. Landaverde, C. Burns, J. Shaw, Z. Garib, J. Andre, E. Blackman, C. J. Freeman, J. Jorba, R. Sutter, G. Tambini, L. Venczel, C. Pedreira, F. Laender, H. Shimizu, T. Yoneyama, T. Miyamura, H. van Der Avoort, M. S. Oberste, D. Kilpatrick, S. Cochi, M. Pallansch, and C. deq Uadros.** 2002. Outbreak of poliomyelitis in Hispaniola associated with circulating type 1 vaccine-derived poliovirus. Science **296:**356–359.
25. **Kew, O. M., R. W. Sutter, B. K. Nottay, M. J. McDonough, D. R. Prevots, L. Quick, and M. A. Pallansch.** 1998. Prolonged replication of a type 1 vaccine-derived poliovirus in an immunodeficient patient. J. Clin. Microbiol. **36:**2893–2899.
26. **Kimura, M.** 1980. A simple method for estimating evolutionary rates of base substitutions through comparative studies of nucleotide sequences. J. Mol. Evol. **16:**111–120.
27. **Lindberg, A. M., P. Andersson, C. Savolainen, M. N. Mulders, and T. Hovi.** 2003. Evolution of the genome of human enterovirus B: incongruence between phylogenies of the VP1 and 3CD regions indicates frequent recombination within the species. J. Gen. Virol. **84:**1223–1235.
28. **Liu, H. M., D. P. Zheng, L. B. Zhang, M. S. Oberste, O. M. Kew, and M. A. Pallansch.** 2003. Serial recombination during circulation of type 1 wild-vaccine recombinant polioviruses in China. J. Virol. **77:**10994–11005.
29. **Lole, K. S., R. C. Bollinger, R. S. Paranjape, D. Gadkari, S. S. Kulkarni, N. G. Novak, R. Ingersoll, H. W. Sheppard, and S. C. Ray.** 1999. Full-length human immunodeficiency virus type 1 genomes from subtype C-infected seroconverters in India, with evidence of intersubtype recombination. J. Virol. **73:**152–160.
30. **Lukashev, A. N., V. A. Lashkevich, O. E. Ivanova, G. A. Koroleva, A. E. Hinkkanen, and J. Ilonen.** 2003. Recombination in circulating enteroviruses. J. Virol. **77:**10423–10431.
31. **Macadam, A. J., C. Arnold, J. Howlett, A. John, S. Marsden, F. Taffs, P. Reeve, N. Hamada, K. Wareham, J. Almond, N. Cammack, and P. D. Minor.** 1989. Reversion of the attenuated and temperature-sensitive phenotypes of the Sabin type 3 strain of poliovirus in vaccinees. Virology **172:**408–414.
32. **MacLennan, C., G. Dunn, A. P. Huissoon, D. S. Kumararatne, J. Martin, P. O'Leary, R. A. Thompson, H. Osman, P. Wood, P. Minor, D. J. Wood, and D. Pillay.** 2004. Failure to clear persistent vaccine-derived neurovirulent poliovirus infection in an immunodeficient man. Lancet **363:**1509–1513.
33. **Mendelsohn, C. L., E. Wimmer, and V. R. Racaniello.** 1989. Cellular recep-

tor for poliovirus: molecular cloning, nucleotide sequence, and expression of a new member of the immunoglobulin superfamily. Cell **56**:855–865.
34. **Minor, P. D.** 1992. The molecular biology of polio vaccines. J. Gen. Virol. **73**:3065–3077.
35. **Nkowane, B. M., S. G. Wassilak, W. A. Orenstein, K. J. Bart, L. B. Schonberger, A. R. Hinman, and O. M. Kew.** 1987. Vaccine-associated paralytic poliomyelitis. United States: 1973 through 1984. JAMA **257**:1335–1340.
36. **Oberste, M. S., K. Maher, D. R. Kilpatrick, and M. A. Pallansch.** 1999. Molecular evolution of the human enteroviruses: correlation of serotype with VP1 sequence and application to picornavirus classification. J. Virol. **73**:1941–1948.
37. **Oberste, M. S., W. A. Nix, K. Maher, and M. A. Pallansch.** 2003. Improved molecular identification of enteroviruses by RT-PCR and amplicon sequencing. J. Clin. Virol. **26**:375–377.
38. **Oberste, M. S., S. Penaranda, and M. A. Pallansch.** 2004. RNA recombination plays a major role in genomic change during circulation of coxsackie B viruses. J. Virol. **78**:2948–2955.
39. **Olive, D. M., S. Al-Mufti, W. Al-Mulla, M. A. Khan, A. Pasca, G. Stanway, and W. Al-Nakib.** 1990. Detection and differentiation of picornaviruses in clinical samples following genomic amplification. J. Gen. Virol. **71**:2141–2147.
40. **Paul, A. V., E. Rieder, D. W. Kim, J. H. van Boom, and E. Wimmer.** 2000. Identification of an RNA hairpin in poliovirus RNA that serves as the primary template in the in vitro uridylylation of VPg. J. Virol. **74**:10359–10370.
41. **Rakoto-Andrianarivelo, M., D. Rousset, R. Razafindratsimandresy, S. Chevaliez, S. Guillot, J. Balanant, and F. Delpeyroux.** 2005. High frequency of human enterovirus species C circulation in Madagascar. J. Clin. Microbiol. **43**:242–249.
42. **Robbins, F. C., and C. A. de Quadros.** 1997. Certification of the eradication of indigenous transmission of wild poliovirus in the Americas. J. Infect. Dis. **175**:S281–S285.
43. **Rotbart, H. A.** 1990. Enzymatic RNA amplification of the enteroviruses. J. Clin. Microbiol. **28**:438–442.
44. **Sabin, A. B.** 1965. Oral poliovirus vaccine. History of its development and prospects for eradication of poliomyelitis. JAMA **194**:872–876.
45. **Saitou, N., and M. Nei.** 1987. The neighbor-joining method: a new method for reconstructing phylogenetic trees. Mol. Biol. Evol. **4**:406–425.
46. **Salk, J. E.** 1960. Persistence of immunity after administration of formalin-treated poliovirus vaccine. Lancet **ii**:715–723.
47. **Savolainen, C., P. Laine, M. N. Mulders, and T. Hovi.** 2004. Sequence analysis of human rhinoviruses in the RNA-dependent RNA polymerase coding region reveals large within-species variation. J Gen. Virol. **85**:2271–2277.
48. **Semler, B. L., and E. Wimmer.** 2002. Molecular biology of picornavirus, p. 387. ASM Press, Washington, D.C.
49. **Shimizu, H., B. Thorley, F. J. Paladin, K. A. Brussen, V. Stambos, L. Yuen, A. Utama, Y. Tano, M. Arita, H. Yoshida, T. Yoneyama, A. Benegas, S. Roesel, M. Pallansch, O. Kew, and T. Miyamura.** 2004. Circulation of type 1 vaccine-derived poliovirus in the Philippines in 2001. J. Virol. **78**:13512–13521.
50. **World Health Organization.** 2004. Polio laboratory manual, 4th ed. W.H.O./IVB/04.10. World Health Organization, Geneva, Switzerland.
51. **Yang, C. F., T. Naguib, S. J. Yang, E. Nasr, J. Jorba, N. Ahmed, R. Campagnoli, H. van der Avoort, H. Shimizu, T. Yoneyama, T. Miyamura, M. Pallansch, and O. Kew.** 2003. Circulation of endemic type 2 vaccine-derived poliovirus in Egypt from 1983 to 1993. J. Virol. **77**:8366–8377.
52. **Yoshida, H., H. Horie, K. Matsuura, and T. Miyamura.** 2000. Characterisation of vaccine-derived polioviruses isolated from sewage and river water in Japan. Lancet **356**:1461–1463.

JOURNAL OF VIROLOGY, Oct. 2005, p. 12623–12634 Vol. 79, No. 20
0022-538X/05/$08.00+0 doi:10.1128/JVI.79.20.12623–12634.2005

Intratypic Recombination among Lineages of Type 1 Vaccine-Derived Poliovirus Emerging during Chronic Infection of an Immunodeficient Patient

Chen-Fu Yang,[1] Hour-Young Chen,[2] Jaume Jorba,[1] Hui-Chih Sun,[2] Su-Ju Yang,[1] Hsiang-Chi Lee,[2] Yhu-Chering Huang,[3] Tzou-Yien Lin,[3] Pei-Jer Chen,[4] Hiroyuki Shimizu,[5] Yorihiro Nishimura,[5] Andi Utama,[5]† Mark Pallansch,[1] Tatsuo Miyamura,[5] Olen Kew,[1] and Jyh-Yuan Yang[2]*

Division of Viral and Rickettsial Diseases, National Center for Infectious Diseases, Centers for Disease Control and Prevention, Atlanta, Georgia 30333[1]; Division of Research and Diagnostics, Center for Disease Control, Taipei, Taiwan 115[2]; Division of Pediatric Infectious Diseases, Chang Gung Children's Hospital, Taoyuan, Taiwan[3]; Graduate Institute of Clinical Medicine, National Taiwan University, Taipei, Taiwan 110[4]; and Department of Virology II, National Institute of Infectious Diseases, Tokyo 208-0011, Japan[5]

Received 27 April 2005/Accepted 20 July 2005

We determined the complete genomic sequences of nine type 1 immunodeficient vaccine-derived poliovirus (iVDPV) isolates obtained over a 337-day period from a poliomyelitis patient from Taiwan with common variable immunodeficiency. The iVDPV isolates differed from the Sabin type 1 oral poliovirus vaccine (OPV) strain at 1.84% to 3.15% of total open reading frame positions and had diverged into at least five distinct lineages. Phylogenetic analysis suggested that the chronic infection was initiated by the fifth and last OPV dose, given 567 days before onset of paralysis, and that divergence of major lineages began very early in the chronic infection. Key determinants of attenuation in Sabin 1 had reverted in the iVDPV isolates, and representative isolates of each lineage showed increased neurovirulence for PVR-Tg21 transgenic mice. None of the isolates had retained the temperature-sensitive phenotype of Sabin 1. All isolates were antigenic variants of Sabin 1, having multiple amino acid substitutions within or near neutralizing antigenic sites 1, 2, and 3a. Antigenic divergence of the iVDPV variants from Sabin 1 followed two major independent evolutionary pathways. The emergence of distinct coreplicating lineages suggests that iVDPVs can replicate for many months at separate sites in the gastrointestinal tract. Some isolates had mosaic genome structures indicative of recombination across and within lineages. iVDPV excretion apparently ceased after 30 to 35 months of chronic infection. The appearance of a chronic VDPV excretor in a tropical, developing country has important implications for the strategy to stop OPV immunization after eradication of wild polioviruses.

The central strategy of the World Health Organization Global Polio Eradication Initiative is widespread use of oral poliovirus vaccine (OPV) at high rates of coverage. This strategy has reduced the global incidence of polio by over 99% since the start of the Initiative in 1988 and restricted wild poliovirus circulation to countries in western and central Africa and southern Asia (87). However, use of OPV is associated with some rare adverse events, including the appearance of cases of vaccine-associated paralytic poliomyelitis among OPV recipients and contacts (76), and the occurrence of polio outbreaks associated with circulating vaccine-derived poliovirus (cVDPV) (36). While cVDPV outbreaks can be prevented by maintenance of high rates of OPV coverage, the occurrence of vaccine-associated paralytic poliomyelitis is associated with the inherent genetic instability of the live, attenuated OPV strains (56).

In immunocompetent individuals, the risk of vaccine-associated paralytic poliomyelitis is very low, estimated in the United States at 1 case per 2.4 million OPV doses distributed (75, 76). The risk of vaccine-associated paralytic poliomyelitis is over 3,000-fold higher in patients with B-cell immunodeficiencies such as common variable immunodeficiency, X-linked agammaglobulinemia, and severe combined immunodeficiency (77). Moreover, whereas the period of poliovirus excretion is usually 2 to 6 weeks in susceptible immunocompetent individuals (2), it can be prolonged for up to 10 years or more in immunodeficient patients (35, 52, 76). Chronic poliovirus excretion (>12 months) appears to be very rare (37) and appears to be largely, but perhaps not exclusively (31, 54), associated with B-cell immunodeficiencies. Fewer than 25 immunodeficient chronic excretors have so far been identified since the introduction of OPV in 1961 (27, 76), and most of the patients have been from high-income countries (27, 76) such as the United States (35, 77), the United Kingdom (52, 53), Germany (5), Italy (11), and Japan (29, 91).

In this report, we describe a case of immunodeficient vaccine-associated paralytic poliomyelitis in a child from Taiwan diagnosed with common variable immunodeficiency (18, 69). The patient was found to have excreted type 1 immunodeficient vaccine-derived polioviruses (iVDPVs) for 10 months after onset of paralysis. From the evolution rate of the iVDPV isolate genomes, we estimated that the total period of excretion was from 30 to 35 months, and that the chronic infection most likely began with administration of the fifth and last dose

* Corresponding author. Mailing address: 161 Kun Yang Street, Nan-Kang District, Taipei, Taiwan 115. Phone: 886-2-2653-1375. Fax: 886-2-2653-0403. E-mail: jyyang@cdc.gov.tw.
† Present address: Research Center for Biotechnology, Bogor, Indonesia.

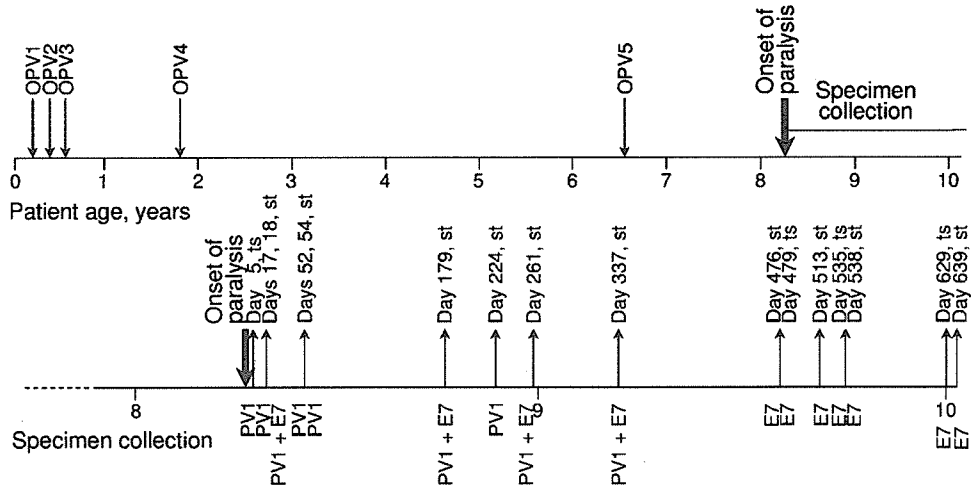

FIG. 1. Time line summarizing immunization history, age at onset of paralysis, and time of specimen collection for the immunodeficient chronic excretor (upper line). The lower line is an expansion of the time line from the patient at age 8 years to 10.1 years showing times (in days after onset of paralysis) of collection of specimens (st, stool specimen; ts, throat swab) found to contain poliovirus type 1 (PV1) iVDPV or echovirus type 7 (E7) or both.

of OPV. The iVDPV isolates obtained from the patient represented five main lineages derived from the common-source infection. All isolates were antigenic variants of the Sabin type 1 OPV strain (LSc 2ab; Sabin 1), but lineages differed in the pattern of amino acid substitution within or near neutralization antigenic sites. Divergence of the separate lineages appeared to have started very early in the chronic infection, with the earliest diverging lineage evolving largely independently. Some iVDPV isolates had mosaic genome structures indicative of recombination across and within lineages. Representative isolates from each lineage were tested for neurovirulence in PVR-Tg21 transgenic mice expressing the human receptor for poliovirus and were found to be either highly or moderately neurovirulent in this animal model. In addition, all isolates when grown in HeLa cells at 39.5°C had lost the temperature-sensitive phenotype of Sabin 1.

There was no evidence of spread of iVDPV to contacts of the case-patient. However, Taiwan currently maintains the high rates of OPV coverage needed to limit iVDPV spread. The appearance of a chronic VDPV excretor in a tropical, developing country underscores the challenges inherent to the development of a global strategy for cessation of OPV use after eradication of wild polioviruses.

MATERIALS AND METHODS

Patient. The case patient, a boy born in 1993, had received a primary series of trivalent OPV doses at ages 2, 4, 6, and 21 months and a booster dose at age 6.7 years (Fig. 1). In April 2001, at age 8 years, the patient developed acute paralysis and was diagnosed with bulbospinal poliomyelitis. Throat swabs and stool specimens were taken for virus culture, and blood specimens were taken for immunologic studies. The patient was diagnosed with common variable immunodeficiency on the basis of quantitative serum immunoglobulin readings and was placed on intravenous immunoglobulin therapy (47).

Virus isolation and typing. Clinical specimens obtained from the case patient included throat swabs taken at 5, 479, 535, and 629 days after onset of paralysis, and stool specimens taken at 17, 18, 52, 54, 179, 224, 261, 337, 476, 513, 538, 639, 688, and 752 days after onset. Stool specimens were also obtained from 62 contacts, including four siblings of the case patient. Virus was isolated by culture in RD (human rhabdomyosarcoma cell line; ATCC CCL 136), L20B (mouse L cells expressing the human poliovirus receptor) (65), and HEp-2 (human cervical carcinoma cell line; ATCC CCL 23) cells (86). Echovirus type 7 (E7) isolates were initially identified by patterns of neutralization with Lim Benyesh-Melnick pools and confirmed by neutralization with E7-specific antisera and VP1 sequencing (86). Poliovirus isolates were initially characterized by immunofluorescence assay, microneutralization, diagnostic PCR (39, 40, 88), and VP1 sequencing (35, 86). Several of the poliovirus isolates had mixed-base sequences at multiple sites, and isolates from specimens taken at days 5, 17, 54, 179, 224, 261, and 337 were plaque purified before complete genomic sequencing.

Antigenic characterization. Initial intratypic differentiation of VDPV isolates used highly specific cross-absorbed antisera in an enzyme-linked immunosorbent assay format (82). Briefly, clinical isolates were tested with two different antiserum preparations, one that reacts with Sabin 1 and another that reacts primarily with wild type 1 polioviruses. In this assay, isolates can have one of four different antigenic properties: (i) vaccine-like (reaction only with the anti-Sabin strain sera), (ii) non-vaccine-like (reaction only with anti-wild poliovirus sera), (iii) double-reactive (reaction with both anti-Sabin strain and anti-wild poliovirus sera), and (iv) nonreactive (no reaction with either anti-Sabin strain or anti-wild poliovirus sera). Only Sabin 1-related isolates have vaccine-like antigenic properties, some Sabin 1-related isolates have double reactive antigenic properties, most wild polioviruses and some Sabin 1-related antigenic variants have non-vaccine-like antigenic properties, and a small number of wild polioviruses and Sabin 1-related antigenic variants have nonreactive antigenic properties (82).

Nucleic acid sequencing. Conditions for reverse transcription-PCR amplification and cycle sequencing were as described previously (50). Sequencing was performed in both directions, and every nucleotide position was sequenced at least once from each strand. Terminal sequences were determined by using the 5′ rapid amplification of cDNA ends (RACE) and 3′ RACE system kits (Life Technologies, Gaithersburg, Md.) according to the manufacturer's instructions.

Phylogenetic analysis. P1/capsid, P2/noncapsid, P3/noncapsid, and complete open reading frame (ORF) sequence relationships among the nine iVDPV isolates and Sabin 1 were constructed from the corresponding regions using the maximum-likelihood method implemented in the DNAml program of the PHYLIP 3.5c package (21). The topology of the trees was obtained by majority-rule consensus among 1,000 bootstrap replicates (20, 21). The corresponding branch lengths were evaluated by likelihood ratio tests among nested models of nucleotide evolution as implemented in the program Modeltest (67). The tree with the best likelihood ratio test score was rooted to the sequences of Sabin 1 and displayed using the program TreeExplorer (K.Tamura, http://evolgen.biol.metro-u.ac.jp/TE/TE_man.html). Insertion/deletion 5′ untranslated region (5′-UTR) differences were treated as single-nucleotide substitutions.

Analysis for recombination across lineages. Discontinuities across different genomic intervals among the day 5, 18, and 52 isolates and among the day 52, 179, and 224 isolates were initially visualized by using distance plot and bootscan functions of the Simplot program (51). The program DnaSP (71) was used to localize the likely sites of recombination by alignment of polymorphic nucleotide sites and analysis of the statistical significance of discontinuities in the extent of

nucleotide sequence identity. Paired estimates of corrected nucleotide substitutions and standard errors among the recombinant sequence blocks were calculated using the MEGA software package (45).

Estimation of the time of the initiating OPV dose. The time of the initiating OPV dose was estimated from the rate of fixation of nucleotide substitutions into the nine iVDPV isolates. The maximum-likelihood estimates of the number of synonymous substitutions at synonymous sites (K_s) that accumulated from the Sabin 1 sequence were computed according to the method of Goldman and Yang (25) as implemented in the CODEML program within the PAML package (90). This method corrects for the transition/transversion rate bias, the codon frequency bias, and for multiple substitutions at a site. Corrected K_s values relative to the root sequence (Sabin 1; K_s set to zero) for each iVDPV isolate were plotted as a function of the date of sample collection. The rate of accumulation of synonymous substitutions was estimated by weighted linear regression (where the weight for each data point was proportional to the reciprocal of the error variance for the corrected K_s value) using statistical applications within the SAS system, version 9 (SAS Institute, Inc., Cary, N.C.). The date of the initiating OPV dose was estimated from the intercept on the abscissa at $K_s = 0$, and the 95% confidence limits around the regression line were calculated following procedures described by Sokal and Rohlf (74).

Estimation of time of divergence of iVDPV lineages. Maximum-likelihood estimates of divergence times were obtained assuming a unique common ancestor and a single linear rate of evolution for all iVDPV lineages, as shown by the linear regression analysis. Under these assumptions, a maximum-likelihood tree was constructed using third codon positions after an exhaustive search (78), and further analyzed under the single rate dated tips model (68) implemented in the PAML package (90) with dated internodes scaled according to the time of the last OPV dose. The parental root sequence was that of the P1/capsid region of Sabin 1 and zero time was assumed to be the date of the last OPV dose (567 days before onset of paralysis).

Numbering of nucleotide and amino acid positions. The ORF sequences of all iVDPV isolates were colinear with those of Sabin 1, but their 5′-UTR sequences were not. To facilitate comparisons, numbering of nucleotide positions of all isolates followed that described for Sabin 1 (59), with insertions assigned serial letters. Amino acid positions were indicated by the name of the viral protein and numbered consecutively from residue 1 of each protein. Amino acid substitutions were indicated by the following convention: viral protein:original residue–position–substituted residue. For example, VP1:T106A indicates a threonine-to-alanine substitution at amino acid position 106 of VP1.

Neurovirulence testing in PVR-Tg21 mice. Neurovirulence tests on iVDPV isolates were carried out on PVR-Tg21 mice as previously described (43, 46, 73). The mice were purchased from the Central Laboratories for Experimental Animals (Kanagawa, Japan). The type 1 reference strains were Mahoney/USA41 (neurovirulent) and Sabin 1 (attenuated). Six or eight mice (equal numbers of males and females) were inoculated (30 μl/mouse) intracerebrally for each virus dilution (in 10-fold increments; range, 1.5 to 7.5 log 50% cell culture infectious dose ($CCID_{50}$)/mouse). Mice were examined daily for 14 days postinoculation, and the times of paralysis or death were recorded. The virus titer that induced paralysis or death in 50% of inoculated mice was calculated by the method of Kärber (32) and expressed as $CCID_{50}$/mouse.

Measurement of temperature-sensitive phenotype. The temperature sensitivity of the iVDPV isolates was measured by the efficiency of plating at 39.5°C compared with 34.5°C. The efficiency of plating values were determined by plaque assays performed on monolayers of HeLa cells as described previously (73, 89).

Nucleotide sequence accession numbers. Complete genomic sequences of the nine iVDPV isolates described in this study were submitted to the GenBank library under accession numbers AF538840, AF538841, AF538842, AF538843, AY928383, AY928384, AY928385, AY928386, and AY928387 (corresponding to the day 5, 17, 52, 337, 261, 224, 54, 179, and 18 isolates, respectively).

RESULTS

Clinical and epidemiologic investigations. The last case of poliomyelitis in Taiwan associated with circulating wild poliovirus occurred in 1982, at the end of a large outbreak (1,043 reported cases with 98 deaths) associated with an imported type 1 poliovirus (13, 41). All subsequent poliovirus isolates obtained since 1982 have been derived from the oral poliovirus vaccine. Taiwan introduced immunization with OPV in 1966 and has maintained high rates of OPV coverage since 1982 and intensive surveillance for cases of acute flaccid paralysis since 1994. In 2000, all countries within the Western Pacific Region of the World Health Organization were certified as polio-free (1, 84).

The case patient developed poliomyelitis in April 2001, 19 years after the last case associated with wild poliovirus in Taiwan. Clinical records indicated that the case patient received five doses of OPV at ages 2, 4, 6, and 21 months and 6.7 years, the last dose given 567 days (~19 months) before onset of paralysis (Fig. 1). At age 8 years, the patient developed fever and upper respiratory tract infection followed by acute left-arm paralysis. Paralysis progressed to his right arm and both legs, and further involved difficulties in swallowing, impairment of tongue and eye movement, and respiratory muscle paralysis. The clinical diagnosis was bulbospinal poliomyelitis. A month after paralysis, the patient was diagnosed with common variable immunodeficiency, a defect in antibody production (18, 69), on the basis of quantitative serum immunoglobulin readings of 270 mg/dl for immunoglobulin G (normal range: 639 to 1,349 mg/dl), 6.2 mg/dl for immunoglobulin M (normal range: 56 to 352 mg/dl), and <5.9 mg/dl for immunoglobulin A (normal range: 70 to 132 mg/dl) (15, 28). He was immediately placed on a therapeutic regimen of monthly injections of intravenous immunoglobulin. The patient continued to have atrophy and residual paralysis in both legs more than 3 years after onset of paralysis.

Clinical specimens were obtained from the patient at days 5 (throat swab), 17, 18, 52, 54, 179, 224, 261, 337, 476, 479 (throat swab), 513, 535 (throat swab), 538, 629 (throat swab), 639, 688, and 752 (all were stool specimens if not otherwise indicated) after onset (Fig. 1). Poliovirus type 1 was isolated from all specimens taken up to day 337. Echovirus type 7 and poliovirus type 1 were isolated from the day 18, 179, 261, and 337 specimens; E7 was isolated from all specimens taken from day 476 to day 639; no virus was isolated from the day 688 and day 752 specimens.

The local bureau of health investigated the polio immunization status of schoolmates of the case patient and children in his neighborhood and community (1,682 children in all). All of the children had been vaccinated with at least 3 doses of OPV, and three contact children under 5 years had received catch-up vaccinations between July and September 2000. In addition, stool specimens were taken from 62 suspected contacts of the case patient (including his four siblings) for virus isolation. None of the contacts were found to be infected with poliovirus.

Sequence properties of poliovirus isolates. Characterization of the early poliovirus isolates (from the days 5, 17, and 18 specimens) by enzyme-linked immunosorbent assay using cross-absorbed neutralizing antisera (82) showed that all were antigenically distinct (nonreactive or non-vaccine-like) from Sabin 1, a property subsequently confirmed for all nine isolates. However, characterization by diagnostic PCR and by sequencing of the VP1 region (906 nucleotides) showed that all isolates were derived from the Sabin 1 strain. The nine isolates differed from Sabin 1 at 2.43% to 3.53% of VP1 nucleotide sequences, from each other at 0.22% (excepting the day 52 and day 54 isolates, which had identical VP1 sequences) to 5.28% of VP1 nucleotide sequences, and from contemporary wild type 1 polioviruses (including representative isolates from the 1982 Taiwan outbreak) at >18% of VP1 nucleotide sequences

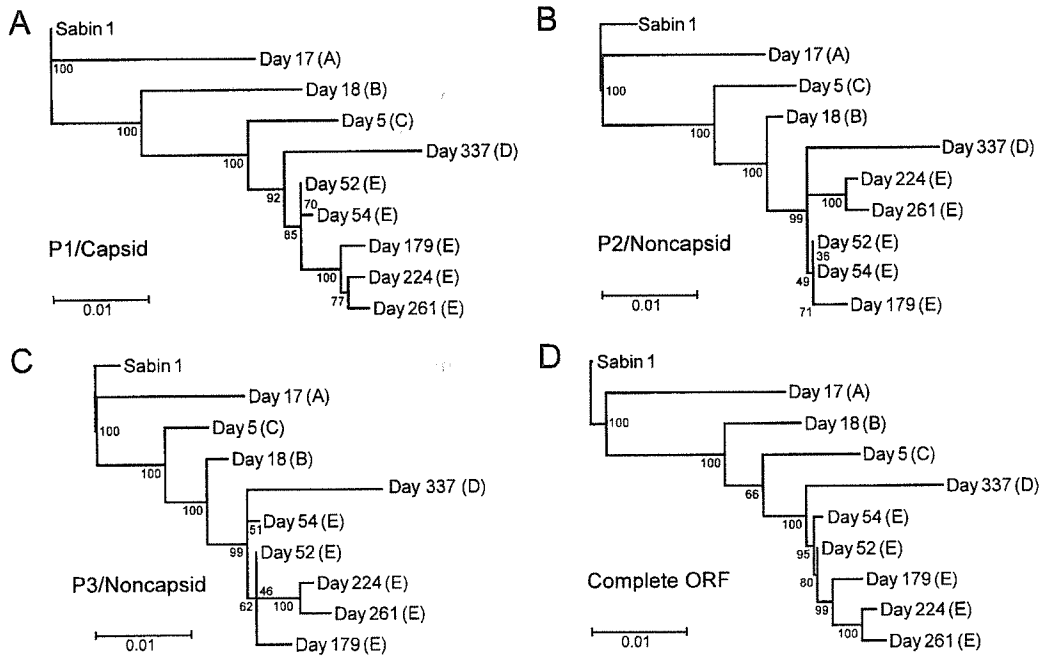

FIG. 2. Maximum-likelihood trees summarizing sequence relationships among the Sabin 1 OPV strain (root of tree) and the nine type 1 iVDPV isolates across different genomic intervals: (A) P1/capsid region (reference interval for evolution rate calculations), (B) P2/noncapsid region, (C) P3/noncapsid region, and (D) complete ORF. Major diverging lineages are labeled A to E.

(34, 73) (data not shown). The Taiwan isolates were identified as iVDPVs in accordance with the World Health Organization classification scheme, where VDPVs are poliovirus clinical isolates having 1% to 15% VP1 nucleotide sequence divergence from the parental OPV strain, and iVDPVs are VDPVs isolated from patients known to have B-cell immunodeficiencies (36).

Subsequent nucleotide sequencing of the complete genomes (7,411 to 7,441 nucleotides) of all nine isolates showed that all sequences were derived from Sabin 1. Most of the genetic differences among isolates were nucleotide substitutions, 82% of which generated synonymous codons. However, three different categories of 5′-UTR deletions were also observed. The day 17 isolate had no 5′-UTR deletions compared to Sabin 1. By contrast, all other VDPV isolates had a deletion of 8 nucleotides at positions 667 to 674, and the day 5 pharyngeal isolate had an additional deletion of 22 nucleotides at positions 695 to 716. The deletions occurred within a highly variable 5′-UTR interval that appears to have little secondary structure (63). Type 1 polioviruses with deletions within this interval have been shown to be viable in cultured cells (24, 44) and in humans (49). Four 5′-UTR nucleotide substitutions (G26A, U344C, U355C, and G480A) were shared by all isolates. All of these substitutions but U344C represent reversions back to the parental Mahoney sequence (59), and all three were consistently found among type 1 cVDPV isolates from Hispaniola (34) and the Philippines (73).

Emergence of multiple iVDPV lineages. Relationships among the complete P1/capsid region sequences of the nine iVDPV isolates were summarized in a tree constructed using the maximum-likelihood algorithm (21) and rooted to the Sabin 1 sequence (Fig. 2A). The tree had a deeply branched topology, with five major branches corresponding to lineages A to E, extending from a single main lineage. The first lineage (A) to branch off from the main lineage is represented by the day 17 isolate. This isolate differed from all others by the absence of any 5′-UTR deletions. Replication of lineage A virus may have ceased soon after onset of paralysis, as no other lineage A isolates were subsequently found. All other isolates contained the 8-nucleotide 5′-UTR deletion, which probably became fixed into the virus population very early in the chronic infection. The P1/capsid sequences of the day 17 (lineage A) and day 18 (lineage B) isolates were quite distinct, differing at 3.9% of nucleotide positions. The extensive divergence of the two isolates was surprising because the viruses originated from stool specimens taken on consecutive days. However, the VP1 sequence of the original day 17 isolate was ambiguous at several positions, indicating that the virus population was a mixture of variants, and the isolate was plaque-purified before complete genomic sequencing. By contrast, the day 18 isolate sequences were unambiguous, so no plaque purification was performed. It is possible that the day 17 specimen also contained lineage B virus that was removed by the plaque-purification step.

The day 18 isolate sequence appears at the tip of a long branch (Fig. 2A), suggesting that the day 18 isolate represents a second lineage that may have terminated soon after onset of paralysis. Two other distinct lineages, C and D, are represented by the day 5 and day 337 isolates, respectively. The 22-nucleotide 5′-UTR deletion apparently occurred after lineage C diverged from the evolutionary pathway leading to lineages D and E. Lineage D is defined by the sequence of the day 337 isolate, from the last poliovirus-positive stool specimen. Lineage E is defined by five closely related isolates from

the day 52, day 54, day 179, day 221, and day 261 specimens. Divergence among isolates of lineage E was limited and probably occurred during the period of sampling.

All sequences of the iVDPV isolates were derived from Sabin 1. Trees of the P2/noncapsid, P3/noncapsid, and complete ORF regions had deeply branched topologies similar to the P1/capsid tree (Fig. 2). However, the four trees were not congruent, as the order of branch nodes and branch lengths differed. For example, the branch nodes of the isolate sequences were ordered day 18 (B) –day 5 (C) –day 337 (D) in the P1/capsid tree, and day 5 (C) –day 18 (B) –day 337 (D) in the P2/noncapsid and P3/noncapsid trees (Fig. 2). Bootstrap support (20, 21) for the order of these nodes was high (>90%) in all trees. Moreover, the branch length of the day 18 isolate from its node was long in the P1/capsid tree and short in the P2/noncapsid and P3/noncapsid trees.

As the window for comparison moved from the P1/capsid region to the P2/noncapsid and P3/noncapsid regions, the branch node of the day 18 isolate shifted away from the root and that of the day 5 isolate shifted toward the root. By contrast, the sequence relationships among most other isolates were similar across the ORF, apart from minor differences in tree topologies that had low bootstrap support. The exception was the day 179 isolate, within lineage E, that was most closely related to the day 224 isolate in the P1/capsid tree, but most closely related to the day 52 isolate in the P2/noncapsid and P3/noncapsid trees. Although some of the differences in tree topologies may be attributable to stochastic variability in the rates of fixation of substitutions across different lineages and genetic intervals, another mechanism probably explains the more pronounced differences.

Recombination across and within iVDPV lineages. Relationships among the aligned complete ORF sequences of the day 5, day 18, and day 52 isolates were initially examined by using the distance plot and bootscan functions of the Simplot program (51), which revealed a possible recombination site between nucleotide positions 2659 and 2678, near the 5′ terminus of the VP1 region (Fig. 3B). Upstream P1/capsid region sequences (nucleotide positions 743 to 2658) of the day 52 isolate more closely matched those of the day 5 isolate (genetic distance 0.006 ± 0.002) than the day 18 isolate (genetic distance 0.035 ± 0.004), whereas the downstream ORF sequences (nucleotide positions 2679 to 7369) of the day 52 isolate more closely matched those of the day 18 isolate (genetic distance 0.007 ± 0.001) than the day 5 isolate (genetic distance 0.019 ± 0.002), a pattern suggestive of recombination.

Because recombination is difficult to detect at low levels of divergence (66), recombination was further investigated using the program DnaSP (71). The sharp discontinuity in the extent of sequence identity, clearly visualized by alignment of polymorphic nucleotide sites among the ORFs of the three isolates (Fig. 3C), was very likely produced by recombination. The likelihood that the observed sequence discontinuities arose by random substitution without recombination is very low ($P < 0.00001$; G test with Williams's correction). Although the summary alignment (Fig. 3B) shows the day 52 isolate genome as a mosaic assembled from upstream sequences similar to those of the day 5 isolate and downstream sequences similar to those of the day 18 isolate, the actual evolutionary relationships among the three isolates is likely to be more complex. For example, runs of sequence differences in the P3/noncapsid regions of the day 18 and day 52 isolates (Fig. 3C) may signal the occurrence of additional recombination events. However, short stretches of recombinant sequences are difficult to distinguish from localized clustering of substitutions (66). More importantly, because the sequences of the parental and progeny viruses directly participating in the recombination events are unknown, and only a small number of representatives of each lineage were available for analysis, the observed mosaic structures of the genomes are explainable by several alternative pathways of recombination.

Similarly, we found that the genome of the day 224 isolate also appeared to be a mosaic, with upstream ORF sequences (nucleotide positions 743 to 3366) more closely related to those of the day 179 isolate and downstream sequences (nucleotide positions 3372 to 7369) more closely related to those of the day 52 isolate (Fig. 3D). Alignment of the polymorphic nucleotide sites (Fig. 3E) revealed discontinuities in the extent of sequence identity that are most likely attributable to recombination ($P = 0.008$ for random substitution without recombination; G test with Williams's correction). The statistical support for recombination among the lineage E isolates was less robust than in the previous example because the number of polymorphic sites distinguishing the ORF sequences of the three isolates was small ($n = 60$).

Estimation of the date of OPV exposure that initiated the chronic iVDPV infection. The topologies of the trees indicated that genetic divergence from Sabin 1 increased with the time of sampling (Fig. 2). An approximately linear relationship ($R^2 = 0.84$) was obtained when the number of synonymous substitutions (K_s) in the P1/capsid region was plotted as a function of the times of collection (zero time: date of last OPV dose) for the nine specimens (Fig. 4). The linear relationship suggests that all lineages were derived from a single OPV dose. The date of the initiating OPV dose, estimated by extrapolation to the time when $K_s = 0$, was 59 days before the fifth and last OPV dose (95% confidence interval: 588 days before to 190 days after the last OPV dose). The rate of P1/capsid evolution estimated from the slope of the regression line was $(2.92 \pm 1.25) \times 10^{-2}$ synonymous substitutions per synonymous site per year, a value very similar to those previously obtained for poliovirus P1/capsid region or VP1 sequences (34, 35, 50, 53). When we performed similar analyses based upon total nucleotide substitutions (K_t) in the P1/capsid region, the intercept was 172 days before the last OPV dose and the evolution rate at all sites was estimated to be $(1.14 \pm 0.45) \times 10^{-2}$ substitutions per site per year (data not shown).

Although the two analyses yielded comparable estimates for the time of start of the chronic infection, we generally prefer to base our estimates upon the rate of fixation of synonymous substitutions, which we assume to accumulate at a nearly constant rate by random genetic drift. We also prefer to use the P1/capsid region for our calculations because it is the largest interval within the ORF that can generally be assumed to share a recent common ancestry, as recombination of noncapsid region sequences with heterologous species C enteroviruses frequently occurs in circulating wild polioviruses (10, 49) and cVDPVs (34, 70, 73, 89). However, because sequences in all genomic intervals were derived from a recent common Sabin 1 ancestor, we were also able to estimate the date of the initiat-

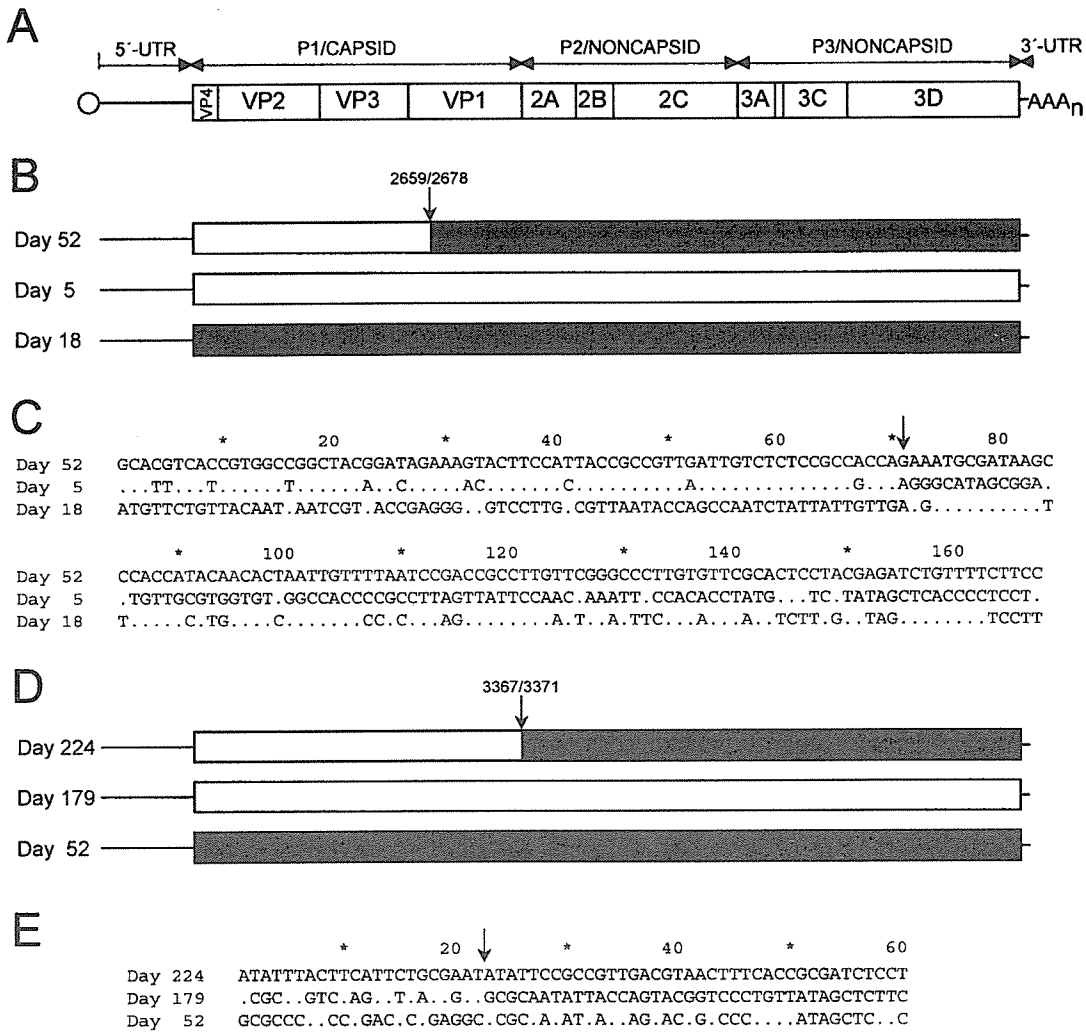

FIG. 3. Recombination across (panels B and C) and within (panels D and E) iVDPV lineages generating mosaic genomes. Panel A: Schematic of the poliovirus genome. The single ORF is represented by a rectangle, flanked by the 5′-UTR and 3′-UTR. Panels B and D: The most recent of the trio of isolates is represented as having the reference mosaic genome, with the sites of sequence discontinuity indicated by arrows. Sequence intervals of the reference mosaic genome most closely matching those of the preceding isolates are shaded accordingly. The 5′-UTR and 3′-UTR sequences were not included in the analyses for recombination and are represented only by lines. Panels C and E: Alignment of ORF nucleotide sites that are polymorphic among each trio of isolates. In each trio, the sequence of the most recent isolate is shown as a reference, with the sequence differences from that reference indicated below for the two preceding isolates. Polymorphic sites are numbered consecutively.

ing dose using the evolutionary rate data for the complete ORF (estimated date: 95 days after the last OPV dose; evolution rate: $[3.70 \pm 0.67] \times 10^{-2}$ synonymous substitutions per synonymous site per year; $R^2 = 0.95$) as well as for VP1 (estimated date: 146 days before the last OPV dose; evolution rate: $[2.41 \pm 1.58] \times 10^{-2}$ synonymous substitutions per synonymous site per year; $R^2 = 0.64$) (data not shown). Recombination across iVDPV lineages would not substantially alter the overall rate estimates provided that all iVDPV lineages evolved at nearly equivalent rates within the same genomic intervals. These evolution rate estimates strongly implicate the fifth and last OPV dose, given 567 days before onset of paralysis, as the OPV exposure event that initiated the chronic iVDPV infection.

Estimated times of divergence of different iVDPV lineages. The topologies of the trees (Fig. 2) suggested that the five major coreplicating iVDPV lineages diverged from each other before or soon after the onset of paralysis. For example, lineage A, whose branch node is near the root in all four trees, apparently diverged from the main lineage very early in the chronic infection. Other lineages diverged subsequently. To estimate the dates of divergence of the major iVDPV lineages, we assumed that all lineages diverged at a single rate of evolution and we used the single rate dated tips model (68) to convert genetic distances into units of time. We further assumed that the chronic infection began with the last OPV dose given 567 days before onset of paralysis. We based our estimates of divergence time upon the sequence relationships within the interval of nucleotides 743 to 2658, the upstream 72% of the P1/capsid region that we assume to have evolved principally by progressive fixation of nucleotide substitutions (Fig. 3B).

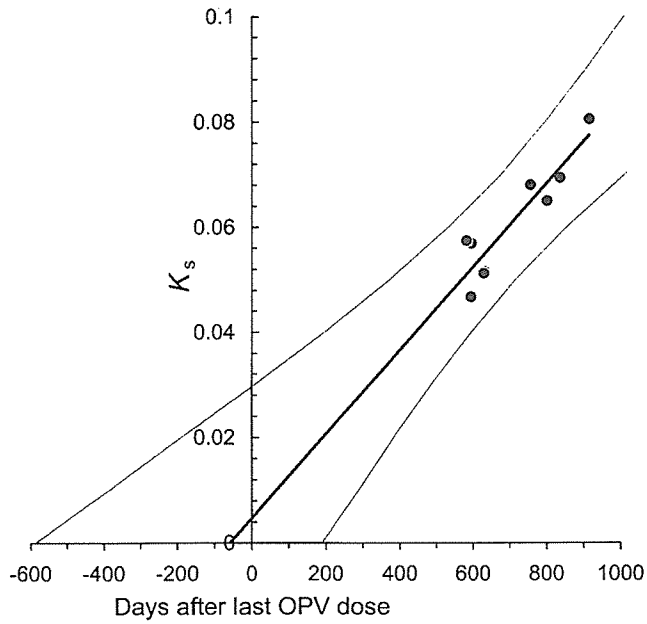

FIG. 4. Estimate of time of the initiating OPV dose from rate of accumulation of synonymous substitutions into the P1/capsid region of the nine type 1 iVDPV isolates. K_s, number of synonymous substitutions at synonymous sites in the P1/capsid region (Sabin 1 sequence set to zero substitutions). The evolution rate was estimated by weighted linear regression (R^2 = 0.84) as described in Materials and Methods. The curves flanking the regression line trace the 95% confidence limits for the time estimates calculated from K_s values.

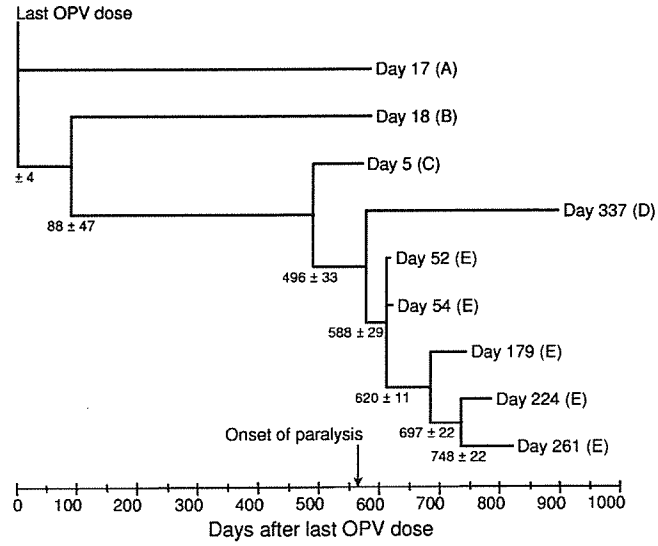

FIG. 5. Estimated times of divergence of major iVDPV lineages based upon the rate of substitution at third-codon positions within the P1/capsid region interval of nucleotides 743 to 2658. Genetic distances and standard errors were scaled under the single rate dated tips model (68) to the time of specimen collection (time zero: date of last OPV dose) as described in Materials and Methods. Note that isolates are identified by the day of specimen collection, not by the day after the last OPV dose.

We obtained a global evolution rate for third codon positions (representing ~91% of all synonymous substitutions) of (3.05 ± 0.34) × 10^{-2} substitutions per site per year for the partial (1916-nucleotide) P1/capsid interval compared. The internal nodes on the phylogenetic tree (Fig. 5) represent point estimates of the times of divergence of lineages A to E during the chronic infection. The topology of the partial P1/capsid tree (Fig. 5) was very similar to that of the complete P1/capsid tree (Fig. 2A) except for differences in the relative branch lengths of lineages B and C. Lineage A was estimated to have diverged from lineages B to E immediately after administration of the last OPV dose. Lineage B diverged from the remaining lineages around day 88, and lineage C around day 496, of the chronic infection. Additional divergences were estimated to have occurred after the onset of paralysis (at day 567 of the chronic infection), with lineages D and E diverging around day 588, and further divergences within lineage E around days 620, 697, and 748 (Fig. 5). Selection of other genomic intervals would have yielded different dates of divergence because of the effects of recombination. However, comparisons across the capsid interval we selected yielded the most deeply branched tree (compare Fig. 2 and 5) and the earliest dates for divergence of lineages A and B. Moreover, most of our phylogenetic comparisons are restricted to P1/capsid region sequences, which encode the defining biological properties of poliovirus (10, 34, 49, 89).

Antigenic divergence of iVDPV lineages. All iVDPV isolates were antigenic variants of the Sabin 1 strain. The day 17 isolate showed non-vaccine-like antigenic properties in the enzyme-linked immunosorbent assay using type-specific cross-absorbed antisera (82), whereas all of the other isolates were nonreactive. The antigenic differences are probably attributable to the numerous amino acid substitutions clustered within or near surface loops forming neutralizing antigenic (NAg) sites 1, 2, and 3a (7, 55, 62) (Fig. 6). Multiple (three to six) amino acid substitutions mapped to the interval forming most of NAg-1 (residues VP1:95 to 106, B–C loop), 1 to 2 substitutions in NAg-2 (at residue VP2:65, E–F loop; and residue VP1:222, G–H loop), and 1 to 4 substitutions within or near NAg-3 (at residues VP3:58 to 60, and VP3:75; loop preceding the B strand). All isolates had amino acid substitutions at site VP3:K060. Substitution at that site is associated with the antigenic reversion (from vaccine-like to non-vaccine-like) of Sabin 1-derived isolates tested with neutralizing monoclonal antibodies (7).

No substitutions were found in surface residues of NAg-3b (VP2:T72 and VP3:P76) or in parts of NAg-2 (VP2:270) and NAg-3a (VP1:287 to 292) (55, 62) (Fig. 6). Four of the substitutions (VP2:D165N, VP1:K99T, VP1:T106A, and VP1:A222T) restored the amino acid of the parental Mahoney strain, and four other substitutions (VP2:D165G, VP3:A59E, VP3:K60Q, and VP1:N100S) were identical to the monoclonal antibody escape mutations that were originally used to define the NAg sites of Sabin 1 (62, 83). The trypsin cleavage site in NAg-1 (VP1:K99), characteristic of Sabin 1 (22), was consistently eliminated by amino acid substitution (day 5 isolate, VP1:K99M; days 18 to 337 isolates, VP1:K99T) in all but the day 17 isolate. Amino acid substitutions outside of the surface loops were generally conservative and mapped to β-sheet structures.

The NAg sites of the day 17 isolate (lineage A; non-vaccine-

	VP2			VP3			VP1		
	NAg3b	NAg2	NAg2	NAg3a	NAg3a	NAg3b	NAg1	NAg2	NAg3a
	71	164 .	269.	56 .	70		95 .	221	287 .
Sabin 1	WTK	DDNQTSPARR	PRL	DLSAKKK	VRLSDKPHTD		SASTKNKDKLFT	SAALGD	KDGTLT
Day 17 (A)	...	.G.....	...	....S..	.....		.VP.....N...	.....	.....
Day 18 (B)	...	.N.....	...	...EQ..	.....		.V.ATS...Q.A	.....	.....
Day 5 (C)	...	.N.....	...	...EQR.	.....Q....		....M.R..Q.A	.....	.....
Day 337 (D)	...	.N.....	...	...EQ..	.....Q....		...ATS..RQ.A	.T....	.....
Day 52 (E)	...	.N.....	...	...EQR.	.....Q....		.V.ATS...Q.A	.T....	.....
Day 54 (E)	...	.N.....	...	...EQR.	.....Q....		.V.ATS...Q.A	.T....	.....
Day 179 (E)	...	.N.....	...	...EQR.	.....Q....		.V.ATS...Q.A	.T....	.....
Day 224 (E)	...	.N.....	...	...EQR.	.....Q....		.V.ATS...Q.A	.T....	.....
Day 261 (E)	...	.N.....	...	...EQR.	.....Q....		.V.ATS...Q.A	.T....	.....
Mahoney	...	.N.....	...	....T..	.....		P...T.....A	.T....	.....

FIG. 6. Sequences of amino acid residues within or bounding neutralizing antigenic sites 1 (VP1:95 to 106), 2 (VP2:164 to 173; VP2:269 to 271; VP1:221 to 226), 3a (VP3:56 to 62; VP3:70 to 74; VP1:287 to 292), and 3b (VP2:71 to 73; VP3:75 to 79). Residues defining the type 1 poliovirus neutralizing antigenic sites by mutations conferring resistance to neutralization by monoclonal antibodies (7, 55, 62, 83) are indicated by boldface type. The trypsin cleavage site in NAg-1 (VP1:K99), characteristic of Sabin 1 (22), is underlined.

like antigenicity) were less highly substituted (5 amino acid substitutions) than those of all other iVDPV isolates (9 to 11 amino acid substitutions; nonreactive antigenicities), and only one substitution (VP1:A96V; NAg-1) was shared with any of the other isolates (lineages B and E) (Fig. 6). The non-vaccine-like antigenicity of the day 17 isolate indicates retention of the capacity to bind the anti-wild poliovirus cross-absorbed sera used in the standard enzyme-linked immunosorbent assay intratypic differentiation test (81, 86), a capacity lost by the more highly substituted nonreactive isolates. Lineage A appears to have followed an independent pathway of antigenic divergence from Sabin 1, consistent with its early divergence from the other lineages. The NAg sites of lineages B to E appear to have shared an early common pathway of antigenic divergence from Sabin 1. However, the NAg-1 sequences of the day 5 isolate (lineage C) differed from the lineage B, D, and E isolates at several positions, and may represent another pathway for antigenic evolution within NAg-1. The NAg sites of all five lineage E isolates were identical (Fig. 6), consistent with the view that the antigenic evolution had stabilized in the late stages of the chronic infection.

Neurovirulence of iVDPV isolates in PVR-Tg21 transgenic mice. Sabin 1 is an attenuated derivative of the neurovirulent Mahoney strain (59, 72). Important determinants of the attenuation phenotype in Sabin 1 include nucleotide G480 in the 5′-UTR and amino acid residues VP4:S65 (encoded by U935), VP3:M325 (encoded by A2438), VP1:T106 (encoded by A2795), and VP1:F134 (encoded by U2879) (9, 33). Reversion of the 5′-UTR determinant, G480A, occurred in all iVDPV isolates (Table 1). Reversion of the capsid determinant, VP1:T106A, occurred in eight of the nine isolates, and reversion of another capsid determinant, VP3:M325L, occurred in seven of the nine isolates. Two determinants, VP4:S65 and VP1:F134, did not revert.

Isolates representing each lineage were tested for neurovirulence in PVR-Tg21 transgenic mice expressing the human re-

TABLE 1. Nucleotide and amino acid substitutions at critical determinants of the attenuation and temperature-sensitive phenotypes of Sabin 1 and the corresponding phenotypes of representative Taiwan iVDPV isolates

Virus	Lineage	5′-UTR 480[c]	Viral protein:amino acid position[a,b]						3′-UTR 7441[d]	Log PD_{50}	EOP[e]
			VP4:65[c,d]	VP3:325[c,d]	VP1:88[d]	VP1:106[c]	VP1:134[c]	3D:73[d]			
Sabin 1		G	S	M	A	T	F	H	G	>8.0[f]	0.009
Day 17	A	A	S	M	A	T	F	Y	A	3.7	1.0
Day 18	B	A	S	M	A	A	F	Y	A	3.5	1.0
Day 5	C	A	S	L	A	A	F	Y	A	2.7	1.3
Day 337	D	A	S	L	A	A	F	Y	A	4.8	0.7
Day 52	E	A	S	L	A	A	F	Y	A	5.6	0.8
Day 261	E	A	S	L	A	A	F	Y	G	3.3	1.1
Mahoney		A	A	L	T	A	L	Y	A	2.8	1.0

[a] Amino acid substitutions correspond to the following nucleotide substitutions: VP4:S65A, U935G; VP3:M325L, A2438U; VP1:A88T, G2741A; VP1:T106A, A2795G; VP1:F134L, U2879C; and 3D:H73Y, C6203U.
[b] Amino acid residues at all six critical sites were identical in all five lineage E isolates.
[c] Site of major determinant of attenuation phenotype in Sabin 1.
[d] Site of major determinant of temperature-sensitive phenotype in Sabin 1.
[e] EOP, efficiency of plating, 39.5°C/34.5°C.
[f] The PD_{50} value of the Sabin 1 strain is quoted from previous reports (46, 73).

ceptor for poliovirus (Table 1). All six iVDPV isolates tested were more neurovirulent than Sabin 1, but only the day 5 pharyngeal isolate (lineage C) appeared to be as highly neurovirulent as the reference Mahoney strain. The day 17 (lineage A), day 18 (lineage B), and day 261 (lineage E) isolates were also highly neurovirulent, but the day 337 (lineage D) and day 52 (lineage E) isolates required substantially higher virus titers to induce paralysis or death in the transgenic mice. Surprisingly, the highly neurovirulent day 5 and day 261 isolates had identical alleles at the five critical sites as the less neurovirulent day 52 and day 337 isolates. Moreover, the day 52 isolate appears to be a recombinant between viruses closely related to the day 5 and day 18 isolates, but was markedly less neurovirulent than either (Table 1). These observations suggest that different genetic backgrounds may modify the effects of reversion at critical determinants of the attenuation phenotype, consistent with the composite nature of the determinants of the attenuation phenotype in Sabin 1 (26). As has recently been noted for type 1 cVDPV isolates from the Philippines (73), evolution toward increased neurovirulence is not necessarily irreversible for derivatives of Sabin 1.

Temperature sensitivity of iVDPV isolates. All three Sabin strains have a temperature-sensitive phenotype, producing lower virus yields at supraoptimal temperatures than wild polioviruses (58, 61). Major determinants of the temperature-sensitive phenotype of Sabin 1 include two amino acid residues associated with the attenuation phenotype (VP4:S65 and VP3:M325; see above), and minor determinants include two amino acids not associated with the attenuation phenotype, VP1:A88 (encoded by G2741) and 3D:H73 (encoded by C6203), along with nucleotide G7441 in the 3′-UTR (9, 64). As described above, the determinant of the temperature-sensitive (and attenuation) phenotypes, VP4:S65, did not revert, whereas the determinant VP3:M325 reverted in all but two iVDPV isolates (Table 1).

Another capsid determinant of the temperature-sensitive phenotype, VP1:A88, also did not revert. By contrast, reversions 3D:H73Y and G7441A occurred in all nine isolates, but an A7441G backmutation restored the Sabin 1 allele in the day 261 isolate. Despite the incomplete reversion at all sites conferring the temperature-sensitive phenotype, plaque yields in HeLa cells for the nine iVDPV isolates were similar at 39.5°C and 34.5°C (Table 1). Under our experimental conditions, the iVDPV isolates were like the Mahoney strain and unlike the temperature-sensitive Sabin 1 strain, which had a ~100-fold decrease in plaque counts at the elevated temperature (Table 1). Thus, the type 1 iVDPV isolates from Taiwan resembled the type 1 cVDPV isolates from Hispaniola (34) and the Philippines (73), which had also lost both the attenuation and temperature-sensitive phenotypes.

DISCUSSION

The genetic relationships among the type 1 iVDPV isolates described in this report highlight the dynamics of poliovirus evolution during chronic infection of an immunodeficient person. At least five distinct type 1 iVDPV lineages, derived from a single initiating OPV dose, emerged over the estimated 30 months of the chronic infection. Divergence of separate lineages began at the start of the infection and continued for at least 18 months thereafter. The five main lineages observed represent the minimum that may have emerged during the chronic infection, as some lineages may have terminated before the collection of the first clinical specimen, estimated to have been taken ~19 months after the start of the chronic infection. Moreover, only nine isolates were obtained over 337 days after onset of paralysis, and all but two of the isolates had been plaque purified before sequencing, so that any potentially wider diversity of the viruses in the original clinical specimens may have escaped detection.

Genetic divergence was associated with changes in the antigenic surface of the viruses. Antigenic evolution of the first diverging lineage (lineage A) appeared to be less extensive than, and independent of, the evolution of the other lineages. Antigenic evolution of lineages B to E followed a common early pathway, with an initial burst of substitutions in or near NAg sites 1, 2, and 3a that probably occurred within the first 3 months of the chronic infection. Antigenic evolution of lineages B, D, and E apparently stabilized afterwards, as only four polymorphic amino acid residues were found among the NAg sites of these lineages, and the antigenic surface of all lineage E isolates apparently remained unchanged during the 209 days of replication from day 52 to day 261. By contrast, the NAg-1 sequences of the day 5 isolate (lineage C) differed from the lineage B and E isolates at five sites, possibly signaling the existence of a diverging pathway for antigenic evolution.

Extensive genetic and antigenic diversity may be a characteristic feature of iVDPV isolates from long-term chronic poliovirus excretors. Stool specimens from other immunodeficient patients with prolonged infections have also been shown to contain mixtures of divergent iVDPV variants (29, 35, 53; R. Park, unpublished data). By contrast, the genetic diversity of vaccine-related or wild poliovirus isolates from immunocompetent individuals is typically low, presumably because the duration of each infection is short. cVDPV isolates from outbreaks similarly have low genetic diversity, as the duration of their infections and modes of transmission are probably the same as for wild polioviruses (34, 70, 73, 89). Although some diversification of wild type 3 poliovirus in a single immunocompetent person has been reported, the extent of divergence was far lower than what has been observed with immunodeficient long-term chronic excretors (42).

The emergence of divergent lineages suggests that the iVDPV had established separate sites of replication within the gastrointestinal tract. Poliovirus replicates in the lymphoid tissue of the oropharynx (tonsils), the small intestine (the Peyer's patches in the ileum), and in the mesenteric lymph nodes (8). The isolation of virus from both throat swabs and stool specimens is indicative of prolonged iVDPV replication in both the oropharynx and in the intestinal tract. It is interesting that the day 5 throat isolate (lineage C) was more closely related to the stool isolates of lineages B, D, and E than was the day 17 stool isolate (lineage A). The deep branch structure of the tree suggests that the separate lineages could replicate independently for extended periods of time (for at least 19 months in the case of lineage A virus). However, the detection of recombination across lineages indicates that the tissue compartmentalization of different lineages was incomplete. It is possible that recombination within and across lineages occurs frequently, but it is difficult to distinguish recombinants from

multiple substitution mutants if the parental viruses are very closely related. Such recombinants become even more difficult to recognize if the intervals exchanged are short or if multiple rounds of genetic exchange had occurred.

Although the patient was concurrently infected with E7 for many months, there was no evidence of genetic exchange between the two coinfecting enteroviruses. The lack of genetic exchange may be attributable to barriers to recombination between human enteroviruses of species B (E7) and species C (including polioviruses) (10, 60). Like the iVDPVs, the E7 isolates also showed evidence of extensive evolution and establishment of separate lineages (J.-Y. Yang, unpublished results).

The occurrence of chronic iVDPV infections may permit observation of processes that normally occur during acute poliovirus infections, but are otherwise undetectable because of the short duration of those infections. For example, intertypic recombination among the three Sabin strains is well documented (12, 23, 48) and frequently occurs in immunocompetent individuals fed trivalent OPV (17, 38), but natural intratypic recombination among OPV variants has been more difficult to demonstrate. Recently, Cherkasova et al. presented evidence consistent with intratypic recombination between coevolving lineages of virus derived from Sabin 2 (14). It is likely that intratypic recombination occurs constantly during natural poliovirus infections, as it does under experimental conditions in cell culture (16). Consistent with experimental findings (80), it is also likely that intratypic recombination in humans occurs at much higher frequencies than intertypic recombination. Similarly, it has long been known that polioviruses can colonize different sites in the gastrointestinal tract, as evidenced by the frequent isolation of virus both from stool specimens and throat swabs taken from the same immunocompetent patient. However, most poliovirus infections are cleared before the emergence of multiple variant lineages becomes evident.

Chronic poliovirus infections of immunodeficient persons may differ from acute infections involving person-to-person transmission of polioviruses in other respects. For example, the NAg sites of circulating wild polioviruses and cVDPVs appear to be more stable than those of iVDPVs from chronic excretors. The well-documented antigenic lability of the Sabin OPV strains (55, 58, 82) appears to only partially account for these differences (J. Jorba et al., unpublished results). Fluctuating antibody levels during immunoglobulin therapy may be an important contributing factor for the rapid antigenic evolution of iVDPVs.

The dynamics of genetic and phenotypic variation described here for iVDPVs are analogous to processes that typically occur during chronic infections established by other rapidly evolving viruses, among which human immunodeficiency virus type 1 has been the most extensively studied. Underlying mechanisms for the rapid evolution of human immunodeficiency virus type 1 in chronically infected patients include the emergence of multiple virus lineages, the proliferation of antigenic variants, the localization of different lineages to separate tissue compartments, and recombination across lineages (57, 92).

The two categories of VDPVs present different risks for the World Health Organization strategy to cease OPV use after global eradication of wild polioviruses (4, 19). The emergence and spread of cVDPVs can be prevented by maintenance of high rates of poliovirus vaccine coverage (36). By contrast, the emergence of iVDPVs in immunodeficient patients is rare and sporadic (27, 37) and cannot be prevented by high levels of population immunity to polioviruses. The potential for person-to-person spread of iVDPVs is unknown, because most iVDPV infections detected so far have occurred in well-immunized communities, and secondary infections have rarely been detected. It is possible that the Taiwan iVDPV had spread to close contacts but that all infections had cleared by the time the immunodeficient patient showed signs of paralysis and the case was investigated. It appears likely that iVDPVs can spread to contacts at least as efficiently as virus excreted by many healthy OPV recipients (6, 75). However, it is unknown whether iVDPVs have the same transmissibility as cVDPVs, which appear to be biologically indistinguishable from wild polioviruses (34, 70, 73, 89).

The risks of emergence of long-term chronic iVDPV excretors vary in different settings (4). Many high-income countries in Europe and North America have shifted from OPV to IPV, thereby effectively preventing the emergence of new vaccine-associated paralytic poliomyelitis cases and iVDPV infections (3). The survival rates of patients with B-cell immunodeficiencies are highest in high-income countries because of the availability of supportive immunoglobulin therapy. In such settings, the occurrence of chronic iVDPV infections is rare even among patients with B-cell immunodeficiencies, and most chronically infected patients either spontaneously cease iVDPV excretion or die from complications of their immunodeficiency (37). Nonetheless, some patients in high-income countries appear to have been infected with iVDPVs for up to 10 years or more and either experienced the late onset of paralytic poliomyelitis (5, 35) or remained asymptomatic carriers of iVDPVs (52).

Although most reports of chronic iVDPV excretors have come from high-income countries (5, 11, 29, 35, 37, 52, 53), recent reports of iVDPV infections have come from other middle-income countries such as Argentina (30), Thailand (79), and Peru (85). Middle-income countries with improving levels of sanitation and rising access to medical care may be at increasing (although very low) risk for the occurrence of immunodeficient chronic iVDPV excretors. This risk will continue as long as OPV is used. By contrast, lower-income countries appear to be at the lowest risk for the occurrence of immunodeficient chronic iVDPV excretors because conditions do not favor the survival of persons with B-cell immunodeficiencies (27). It thus appears especially important for middle- and high-income countries that improved methods for detecting iVDPV infections be developed and that effective therapies for clearing chronic poliovirus infections be found.

ACKNOWLEDGMENTS

We thank Tsan-Chang Tseng and Tsuey-Li Lin (Taiwan CDC) and Ray Campagnoli, Naomi Dybdahl-Sissoko, Deborah Moore, Annelet Vincent, and A. J. Williams (CDC, Atlanta) for excellent technical assistance.

This work was supported, in part, by grants from the National Research Program for Genomic Medicine (93-0324-19-F-00-00-00-35), National Science Council, Taiwan; Center for Disease Control Research Project (DOH91-DC-2022), Department of Health, Taiwan; and by grants-in-aid for Promotion of Polio Eradication from the Ministry of Health, Labor and Welfare, Japan. H.S. was supported, in

part, by grants-in-aid for Development of Expanded Programme on Immunization and Accelerating Measles Control in the Polio-free Era from the Ministry of Health, Labor and Welfare, Japan. A.U. was supported by grants-in-aid from the Japan Society for the Promotion of Sciences.

REFERENCES

1. **Adams, T.** 2000. Farewell to polio in the Western Pacific. Bull. W.H.O. **78:**1375.
2. **Alexander, J. P., Jr., H. E. Gary, Jr., and M. A. Pallansch.** 1997. Duration of poliovirus excretion and its implications for acute flaccid paralysis surveillance: a review of the literature. J. Infect. Dis. **175**(Suppl. 1):S176–S182.
3. **Alexander, L. N., J. F. Seward, T. A. Santibanez, M. A. Pallansch, O. M. Kew, D. R. Prevots, P. M. Strebel, J. Cono, M. Wharton, W. A. Orenstein, and R. W. Sutter.** 2004. Vaccine policy changes and epidemiology of poliomyelitis in the United States. JAMA **292:**1696–1701.
4. **Aylward, R. B., and S. L. Cochi.** 2004. Framework for evaluating the risks of paralytic poliomyelitis after global interruption of wild poliovirus transmission. Bull. W.H.O. **82:**40–46.
5. **Bellmunt, A., G. May, R. Zell, P. Pring-Akerblom, W. Verhagen, and A. Heim.** 1999. Evolution of poliovirus type I during 5.5 years of prolonged enteral replication in an immunodeficient patient. Virology **265:**178–184.
6. **Benyesh-Melnick, M., J. L. Melnick, W. E. Rawls, I. Wimberley, J. Barrera-Oro, E. Ben-Porath, and V. Rennick.** 1967. Studies on the immunogenicity, communicability, and genetic stability of oral poliovaccine administered during the winter. Am. J. Epidemiol. **86:**112–136.
7. **Blondel, B., R. Crainic, O. Fichot, G. Dufraisse, A. Candréa, D. Diamond, M. Girard, and F. Horaud.** 1986. Mutations conferring resistance to neutralization with monoclonal antibodies in type 1 poliovirus can be located outside or inside the antibody-binding site. J. Virol. **57:**81–90.
8. **Bodian, D., and D. M. Horstmann.** 1965. Polioviruses, p. 430–473. *In* F. L. Horsfall and I. Tamm (ed.), Viral and rickettsial infections of man, 4th ed. J. B. Lippincott, Philadelphia, Pa.
9. **Bouchard, M. J., D. H. Lam, and V. R. Racaniello.** 1995. Determinants of attenuation and temperature sensitivity in the type 1 poliovirus Sabin strain. J. Virol. **69:**4972–4978.
10. **Brown, B. A., M. S. Oberste, K. Maher, and M. Pallansch.** 2003. Complete genomic sequencing shows that polioviruses and members of human enterovirus species C are closely related in the non-capsid coding region. J. Virol. **77:**8973–8984.
11. **Buttinelli, G., V. Donati, S. Fiore, J. Marturano, A. Plebani, P. Balestri, A. R. Soresina, R. Vivarelli, F. Delpeyroux, J. Martín, and L. Fiore.** 2003. Nucleotide variation in Sabin type 2 poliovirus from an immunodeficient patient with poliomyelitis. J. Gen. Virol. **84:**1215–1221.
12. **Cammack, N., A. Phillips, G. Dunn, V. Patel, and P. D. Minor.** 1988. Intertypic genomic rearrangements of poliovirus strains in vaccinees. Virology **167:**507–514.
13. **Centers for Disease Control and Prevention.** 1983. Update: poliomyelitis outbreak —Taiwan. Morb. Mortal. Wkly. Rep. **32:**384–386.
14. **Cherkasova, E. A., M. L. Yakovenko, G. V. Rezapkin, E. A. Korotkova, O. E. Ivanova, T. P. Eremeeva, L. I. Krasnoproshina, N. I. Romanenkova, N. R. Rozaeva, L. Sirota, V. I. Agol, and K. M. Chumakov.** 2005. Spread of vaccine-derived poliovirus from a paralytic case in an immunodeficient child: an insight into the natural evolution of oral polio vaccine. J. Virol. **79:**1062–1070.
15. **Conley, M. E., L. D. Notarangelo, and A. Etzioni.** 1999. Diagnostic criteria for primary immunodeficiencies. Clin. Immunol. **93:**190–197.
16. **Cooper, P. D.** 1968. A genetic map of poliovirus temperature-sensitive mutants. Virology **35:**584–596.
17. **Cuervo, N. S., S. Guillot, N. Romanenkova, M. Combiescu, A. Aubert-Combiescu, M. Seghier, V. Caro, R. Crainic, and F. Delpeyroux.** 2001. Genomic features of intertypic recombinant Sabin poliovirus strains excreted by primary vaccinees. J. Virol. **75:**5740–5751.
18. **Cunningham-Rundles, C., and C. Bodian.** 1999. Common variable immunodeficiency: clinical and immunological features of 248 patients. Clin. Immunol. **92:**34–48.
19. **Dowdle, W. R., E. de Gourville, O. M. Kew, M. A. Pallansch, and D. J. Wood.** 2003. Polio eradication: the OPV paradox. Rev. Med. Virol. **13:**277–291.
20. **Felsenstein, J.** 2004. Inferring phylogenies. Sinauer Associates, Sunderland, Mass.
21. **Felsenstein, J.** 1993. PHYLIP (phylogeny inference package), version 3.5c. Department of Genetics, University of Washington, Seattle.
22. **Fricks, C. E., J. P. Icenogle, and J. M. Hogle.** 1985. Trypsin sensitivity of the Sabin strain type 1 poliovirus: cleavage sites in virions and related particles. J. Virol. **54:**856–859.
23. **Furione, M., S. Guillot, D. Otelea, J. Balanant, A. Candrea, and R. Crainic.** 1993. Polioviruses with natural recombinant genomes isolated from vaccine-associated poliomyelitis. Virology **196:**199–208.
24. **Gmyl, A. P., E. V. Pilipenko, S. V. Maslova, G. A. Belov, and V. I. Agol.** 1993. Functional and genetic plasticities of the poliovirus genome: quasi-infectious RNAs modified in the 5′-untranslated region yield a variety of pseudorevertants. J. Virol. **67:**6309–6316.
25. **Goldman, N., and Z. Yang.** 1994. A codon-based model of nucleotide substitution for protein-coding DNA sequences. Mol. Biol. Evol. **11:**725–736.
26. **Gromeier, M., and A. Nomoto.** 2002. Determinants of poliovirus pathogenesis, p. 367–379. *In* B. L. Semler and E. Wimmer (ed.), Molecular biology of picornaviruses. ASM Press, Washington, D.C.
27. **Halsey, N. A., J. Pinto, F. Espinosa-Rosales, M. A. Faure-Fontenia, E. da Silva, A. J. Khan, A. D. B. Webster, P. D. Minor, G. Dunn, E. Asturias, H. Hussain, M. A. Pallansch, O. M. Kew, J. Winkelstein, R. Sutter, and the Polio Project Team.** 2004. Search for poliovirus carriers in persons with primary immune deficiency diseases in the United States, Mexico, Brazil, and the United Kingdom. Bull. W.H.O. **82:**3–8.
28. **Hamilton, R. G.** 1997. Human immunoglobulins, p. 65–109. *In* M. S. Leffell, A. D. Donnenberg, and N. R. Rose (ed.), Handbook of human immunology. CRC Press, Boca Raton, Fla.
29. **Hara, M., Y. Saito, T. Komatsu, H. Kodama, W. Abo, S. Chiba, and T. Nakao.** 1981. Antigenic analysis of polioviruses isolated from a child with agammaglobulinemia and paralytic poliomyelitis after Sabin vaccine administration. Microbiol. Immunol. **25:**905–913.
30. **Hidalgo, S., M. Garcia Erro, D. Cisterna, and M. C. Freire.** 2003. Paralytic poliomyelitis caused by a vaccine-derived polio virus in an antibody-deficient Argentinean child. Pediatr. Infect. Dis. J. **22:**570–572.
31. **Hovi, T., N. Lindholm, C. Savolainen, M. Stenvik, and C. Burns.** 2004. Evolution of wild-type 1 poliovirus in two healthy siblings excreting the virus over a period of 6 months. J. Gen. Virol. **85:**369–377.
32. **Kärber, G.** 1931. Beitrag zur kollektiven Behandlung pharmakologischer Reihenversuche. Arch. Exp. Pathol. Pharmakol. **162:**480–483.
33. **Kawamura, N., M. Kohara, S. Abe, T. Komatsu, K. Tago, M. Arita, and A. Nomoto.** 1989. Determinants in the 5′ noncoding region of poliovirus Sabin 1 RNA that influence the attenuation phenotype. J. Virol. **63:**1302–1309.
34. **Kew, O. M., V. Morris-Glasgow, M. Landaverde, C. Burns, J. Shaw, Z. Garib, J. André, E. Blackman, C. J. Freeman, J. Jorba, R. Sutter, G. Tambini, L. Venczel, C. Pedreira, F. Laender, H. Shimizu, T. Yoneyama, T. Miyamura, H. van der Avoort, M. S. Oberste, D. Kilpatrick, S. Cochi, M. Pallansch, and C. de Quadros.** 2002. Outbreak of poliomyelitis in Hispaniola associated with circulating type 1 vaccine-derived poliovirus. Science **296:**356–359.
35. **Kew, O. M., R. W. Sutter, B. Nottay, M. McDonough, D. R. Prevots, L. Quick, and M. Pallansch.** 1998. Prolonged replication of a type 1 vaccine-derived poliovirus in an immunodeficient patient. J. Clin. Microbiol. **36:**2893–2899.
36. **Kew, O. M., P. F. Wright, V. I. Agol, F. Delpeyroux, H. Shimizu, N. Nathanson, and M. A. Pallansch.** 2004. Circulating vaccine-derived polioviruses: current state of knowledge. Bull. W.H.O. **82:**16–23.
37. **Khetsuriani, N., D. R. Prevots, L. Quick, M. E. Elder, M. Pallansch, O. Kew, and R. W. Sutter.** 2003. Persistence of vaccine-derived polioviruses among immunodeficient persons with vaccine-associated paralytic poliomyelitis. J. Infect. Dis. **188:**1845–1852.
38. **Kilpatrick, D. R., K. Ching, J. Iber, R. Campagnoli, C. J. Freeman, N. Mishrik, M. A. Pallansch, and O. M. Kew.** 2004. Multiplex PCR method for identifying recombinant vaccine-related polioviruses. J. Clin. Microbiol. **42:**4313–4315.
39. **Kilpatrick, D. R., B. Nottay, C.-F. Yang, S.-J. Yang, E. da Silva, S. Peñaranda, M. Pallansch, and O. Kew.** 1998. Serotype-specific identification of polioviruses by PCR using primers containing mixed-base or deoxyinosine residues at positions of codon degeneracy. J. Clin. Microbiol. **36:**352–357.
40. **Kilpatrick, D. R., B. Nottay, C.-F. Yang, S.-J. Yang, M. N. Mulders, B. P. Holloway, M. A. Pallansch, and O. M. Kew.** 1996. Group-specific identification of polioviruses by PCR using primers containing mixed-base or deoxyinosine residues at positions of codon degeneracy. J. Clin. Microbiol. **34:**2990–2996.
41. **Kim-Farley, R. J., G. Rutherford, P. Lichfield, S. T. Hsu, W. A. Orenstein, L. B. Schonberger, K. J. Bart, K. J. Lui, and C. C. Lin.** 1984. Outbreak of paralytic poliomyelitis, Taiwan. Lancet **ii:**1322–1324.
42. **Kinnunen, L., T. Pöyry, and T. Hovi.** 1991. Generation of virus genetic lineages during an outbreak of poliomyelitis. J. Gen. Virol. **72:**2483–2489.
43. **Koike, S., C. Taya, T. Kurata, S. Abe, I. Ise, H. Yonekawa, and A. Nomoto.** 1991. Transgenic mice susceptible to poliovirus. Proc. Natl. Acad. Sci. USA **88:**951–955.
44. **Kuge, S., and A. Nomoto.** 1987. Construction of viable deletion and insertion mutants of the Sabin strain of type 1 poliovirus: function of the 5′ noncoding sequence in viral replication. J. Virol. **61:**1478–1487.
45. **Kumar, S., K. Tamura, I. B. Jakobsen, and M. Nei.** 2001. MEGA2: molecular evolutionary genetic analysis software. Bioinformatics **17:**1244–1245.
46. **Li, J., L.-B. Zhang, T. Yoneyama, H. Yoshida, H. Shimizu, K. Yoshii, M. Hara, T. Nomura, H. Yoshikura, T. Miyamura, and A. Hagiwara.** 1996. Genetic basis of the neurovirulence of type 1 polioviruses isolated from vaccine-associated paralytic patients. Arch. Virol. **141:**1047–1054.
47. **Lin, S.-J., H.-C. Chao, K.-W. Chang, and D.-C. Yan.** 2003. Effect of interleukin 15 and interleukin 2 on anti-CD3-induced T-cell activation and apo-

ptosis in children with common variable immunodeficiency. Ann. Allergy Asthma Immunol. **91**:65–70.
48. **Lipskaya, G. Y., A. R. Muzychenko, O. K. Kutitova, S. V. Maslova, M. Equestre, S. G. Drozdov, R. Perez Bercoff, and V. I. Agol.** 1991. Frequent isolation of intertypic poliovirus recombinants with serotype 2 specificity from vaccine-associated polio cases. J. Med. Virol. **35**:290–296.
49. **Liu, H.-M., D.-P. Zheng, L.-B. Zhang, M. S. Oberste, O. M. Kew, and M. A. Pallansch.** 2003. Serial recombination during circulation of type 1 wild-vaccine recombinant polioviruses in China. J. Virol. **77**:10994–11005.
50. **Liu, H.-M., D.-P. Zheng, L.-B. Zhang, M. S. Oberste, M. A. Pallansch, and O. M. Kew.** 2000. Molecular evolution of a type 1 wild-vaccine poliovirus recombinant during widespread circulation in China. J. Virol. **74**:11153–11161.
51. **Lole, K. S., R. C. Bollinger, R. S. Paranjape, D. Gadkari, S. S. Kulkarni, N. G. Novak, R. Ingersoll, H. W. Sheppard, and S. C. Ray.** 1999. Full-length human immunodeficiency virus type 1 genomes from subtype C-infected seroconverters in India, with evidence of intersubtype recombination. J. Virol. **73**:152–160.
52. **MacLennan, C., G. Dunn, A. P. Huissoon, D. S. Kumararatne, J. Martín, P. O'Leary, R. A. Thompson, H. Osman, P. Wood, P. Minor, D. J. Wood, and D. Pillay.** 2004. Failure to clear persistent vaccine-derived neurovirulent poliovirus infection in an immunodeficient man. Lancet **363**:1509–1513.
53. **Martín, J., G. Dunn, R. Hull, V. Patel, and P. D. Minor.** 2000. Evolution of the Sabin strain of type 3 poliovirus in an immunodeficient patient during the entire 637-day period of virus excretion. J. Virol. **74**:3001–3010.
54. **Martín, J., K. Odoom, G. Tuite, G. Dunn, N. Hopewell, G. Cooper, C. Fitzharris, K. Butler, W. W. Hall, and P. D. Minor.** 2004. Long-term excretion of vaccine-derived poliovirus by a healthy child. J. Virol. **78**:13839–13847.
55. **Minor, P. D.** 1990. Antigenic structure of picornaviruses. Curr. Top. Microbiol. Immunol. **161**:121–154.
56. **Minor, P. D., and J. W. Almond.** 2002. Poliovirus vaccines: molecular biology and immune response, p. 381–390. *In* B. L. Semler and E. Wimmer (ed.), Molecular biology of picornaviruses. ASM Press, Washington, D.C.
57. **Morris, A., M. Marsden, K. Halcrow, E. S. Hughes, R. P. Brettle, J. E. Bell, and P. Simmonds.** 1999. Mosaic structure of the human immunodeficiency virus type 1 genome infecting lymphoid cells and the brain: evidence for frequent in vivo recombination events in the evolution of regional populations. J. Virol. **73**:8720–8731.
58. **Nakano, J. H., M. H. Hatch, M. L. Thieme, and B. Nottay.** 1978. Parameters for differentiating vaccine-derived and wild poliovirus strains. Prog. Med. Virol. **24**:78–206.
59. **Nomoto, A., T. Omata, H. Toyoda, S. Kuge, H. Horie, Y. Kataoka, Y. Genba, Y. Nakano, and N. Imura.** 1982. Complete nucleotide sequence of the attenuated poliovirus Sabin 1 strain genome. Proc. Natl. Acad. Sci. USA **79**:5793–5797.
60. **Oberste, M. S., K. Maher, and M. A. Pallansch.** 2004. Evidence for frequent recombination within species human enterovirus B based on complete genomic sequences of all thirty-seven serotypes. J. Virol. **78**:855–867.
61. **Omata, T., M. Kohara, S. Kuge, T. Komatsu, S. Abe, B. L. Semler, A. Kameda, H. Itoh, M. Arita, E. Wimmer, and A. Nomoto.** 1986. Genetic analysis of the attenuation phenotype of poliovirus type 1. J. Virol. **58**:348–358.
62. **Page, G. S., A. G. Mosser, J. M. Hogle, D. J. Filman, R. R. Rueckert, and M. Chow.** 1988. Three-dimensional structure of poliovirus serotype 1 neutralizing determinants. J. Virol. **62**:1781–1794.
63. **Palmenberg, A. C., and J.-Y. Sgro.** 1997. Topological organization of picornaviral genomes: statistical prediction of RNA structural signals. Semin. Virol. **8**:231–241.
64. **Paul, A. V., J. Mugavero, J. Yin, S. Hobson, S. Schultz, J. H. van Boom, and E. Wimmer.** 2000. Studies on the attenuation phenotype of polio vaccines: poliovirus RNA polymerase derived from Sabin type 1 sequence is temperature sensitive in the uridylylation of VPg. Virology **272**:72–84.
65. **Pipkin, P. A., D. J. Wood, V. R. Racaniello, and P. D. Minor.** 1993. Characterisation of L cells expressing the human poliovirus receptor for the specific detection of polioviruses in vitro. J. Virol. Methods **41**:333–340.
66. **Posada, D.** 2002. Evaluation of methods for detecting recombination from DNA sequences: empirical data. Mol. Biol. Evol. **19**:708–717.
67. **Posada, D., and K. A. Crandall.** 1998. MODELTEST: testing the model of DNA substitution. Bioinformatics **14**:817–818.
68. **Rambaut, A.** 2000. Estimating the rate of molecular evolution: incorporating non-contemporaneous sequences into maximum likelihood phylogenies. Bioinformatics **16**:395–399.
69. **Rosen, F. S., M. D. Cooper, and R. J. P. Wedgwood.** 1995. The primary immunodeficiencies. N. Engl. J. Med. **333**:431–440.
70. **Rousset, D., M. Rakoto-Andrianarivelo, R. Razafindratsimandresy, B. Randriamanalina, S. Guillot, J. Balanant, P. Mauclère, and F. Delpeyroux.** 2003. Recombinant vaccine-derived poliovirus in Madagascar. Emerg. Infect. Dis. **9**:885–887.
71. **Rozas, J., J. C. Sánchez-DelBarrio, X. Messeguer, and R. Rozas.** 2003. DnaSP, DNA polymorphism analyses by the coalescent and other methods. Bioinformatics **19**:2496–2497.
72. **Sabin, A. B., and L. R. Boulger.** 1973. History of Sabin attenuated poliovirus oral live vaccine strains. J. Biol. Stand. **1**:115–118.
73. **Shimizu, H., B. Thorley, F. J. Paladin, K. A. Brussen, V. Stambos, L. Yuen, A. Utama, Y. Tano, M. Arita, H. Yoshida, T. Yoneyama, A. Benegas, S. Roesel, M. Pallansch, O. Kew, and T. Miyamura.** 2004. Circulation of type 1 vaccine-derived poliovirus in the Philippines in 2001. J. Virol. **78**:13512–13521.
74. **Sokal, R. R., and F. J. Rohlf.** 1995. Biometry, 3 ed. W. H. Freeman and Co., New York, NY.
75. **Strebel, P. M., R. W. Sutter, S. L. Cochi, R. J. Biellik, E. W. Brink, O. M. Kew, M. A. Pallansch, W. A. Orenstein, and A. R. Hinman.** 1992. Epidemiology of poliomyelitis in the United States one decade after the last reported case of indigenous wild virus-associated disease. Clin. Infect. Dis. **14**:568–579.
76. **Sutter, R. W., O. M. Kew, and S. L. Cochi.** 2004. Poliovirus vaccine –live, p. 651–705. *In* S. A. Plotkin and W. A. Orenstein (ed.), Vaccines, 4th ed. W.B. Saunders Company, Philadelphia, Pa.
77. **Sutter, R. W., and R. Prevots.** 1994. Vaccine-associated paralytic poliomyelitis among immunodeficient persons. Infect. Med. **11**:426–438.
78. **Swofford, D. L.** 2002. PAUP*: phylogenetic analysis using parsimony (*and other methods), version 4. Sinaeur Associates, Sunderland, Mass.
79. **Tharmaphornpilas, P.** 2005. Vaccine-derived poliovirus, Thailand, 2003. Emerg. Infect. Dis. **11**:777–778.
80. **Tolskaya, E. A., L. I. Romanova, M. S. Kolesnikova, and V. I. Agol.** 1983. Intertypic recombination in poliovirus: genetic and biochemical studies. Virology **124**:121–132.
81. **van der Avoort, H. G., J. H. Reimerink, A. Ras, M. N. Mulders, and A. M. van Loon.** 1995. Isolation of epidemic poliovirus from sewage during the 1992–3 type 3 outbreak in The Netherlands. Epidemiol. Infect. **114**:481–491.
82. **van der Avoort, H. G. A. M., B. P. Hull, T. Hovi, M. A. Pallansch, O. M. Kew, R. Crainic, D. J. Wood, M. N. Mulders, and A. M. van Loon.** 1995. A comparative study of five methods of intratypic differentiation of polioviruses. J. Clin. Microbiol. **33**:2562–2566.
83. **Wiegers, K., H. Uhlig, and R. Dernick.** 1988. Evidence for a complex structure of neutralization antigenic site I of poliovirus type 1 Mahoney. J. Virol. **62**:1845–1848.
84. **World Health Organization.** 2000. Certification of poliomyelitis eradication: Western Pacific Region. Wkly. Epidemiol. Rec. **75**:399–400.
85. **World Health Organization.** 2004. Laboratory surveillance for wild and vaccine-derived polioviruses, January 2003—June 2004. Wkly. Epidemiol. Rec. **79**:393–398.
86. **World Health Organization.** 2004. Polio laboratory manual, 4th ed. World Health Organization, Geneva, Switzerland.
87. **World Health Organization.** 2005. Progress towards interruption of wild poliovirus transmission, January 2004 to March 2005. Wkly. Epidemiol. Rec. **80**:149–155.
88. **Yang, C.-F., L. De, B. P. Holloway, M. A. Pallansch, and O. M. Kew.** 1991. Detection and identification of vaccine-related polioviruses by the polymerase chain reaction. Virus Res. **20**:159–179.
89. **Yang, C.-F., T. Naguib, S.-J. Yang, E. Nasr, J. Jorba, N. Ahmed, R. Campagnoli, H. van der Avoort, H. Shimizu, T. Yoneyama, T. Miyamura, M. A. Pallansch, and O. Kew.** 2003. Circulation of endemic type 2 vaccine-derived poliovirus in Egypt, 1983 to 1993. J. Virol. **77**:8366–8377.
90. **Yang, Z.** 1997. PAML: a program package for phylogenetic analysis by maximum likelihood. Comput. Appl. Biosci. **13**:555–556.
91. **Yoneyama, T., A. Hagiwara, M. Hara, and H. Shimojo.** 1982. Alteration in oligonucleotide fingerprint patterns of the viral genome in poliovirus type 2 isolated from paralytic patients. Infect. Immun. **37**:46–53.
92. **Zhang, L., L. Rowe, T. He, C. Chung, J. Yu, W. Yu, A. Talal, M. Markowitz, and D. D. Ho.** 2002. Compartmentalization of surface envelope glycoprotein of human immunodeficiency virus type 1 during acute and chronic infection. J. Virol. **76**:9465–9473.

JOURNAL OF VIROLOGY, Apr. 2005, p. 4460–4469 Vol. 79, No. 7
0022-538X/05/$08.00+0 doi:10.1128/JVI.79.7.4460–4469.2005

The Alpha/Beta Interferon Response Controls Tissue Tropism and Pathogenicity of Poliovirus

Miki Ida-Hosonuma,[1] Takuya Iwasaki,[2] Tomoki Yoshikawa,[1,3] Noriyo Nagata,[3] Yuko Sato,[3] Tetsutaro Sata,[3] Mitsutoshi Yoneyama,[4] Takashi Fujita,[4] Choji Taya,[5] Hiromichi Yonekawa,[5] and Satoshi Koike[1]*

Department of Microbiology & Immunology,[1] Tokyo Metropolitan Institute for Neuroscience, Department of Tumor Cell Research,[4] and Department of Laboratory Animal Sciences,[5] Tokyo Metropolitan Institute of Medical Sciences, Tokyo Metropolitan Organization for Medical Research, and Department of Pathology, National Institute of Infectious Diseases,[3] Tokyo, and Department of Pathology, Institute of Tropical Medicine, Nagasaki University, Nagasaki,[2] Japan

Received 29 August 2004/Accepted 12 November 2004

Poliovirus selectively replicates in neurons in the spinal cord and brainstem, although poliovirus receptor (PVR) expression is observed in both the target and nontarget tissues in humans and transgenic mice expressing human PVR (PVR-transgenic mice). We assessed the role of alpha/beta interferon (IFN) in determining tissue tropism by comparing the pathogenesis of the virulent Mahoney strain in PVR-transgenic mice and PVR-transgenic mice deficient in the alpha/beta IFN receptor gene (PVR-transgenic/*Ifnar* knockout mice). PVR-transgenic/*Ifnar* knockout mice showed increased susceptibility to poliovirus. After intravenous inoculation, severe lesions positive for the poliovirus antigen were detected in the liver, spleen, and pancreas in addition to the central nervous system. These results suggest that the alpha/beta IFN system plays an important role in determining tissue tropism by protecting nontarget tissues that are potentially susceptible to infection. We subsequently examined the expression of IFN and IFN-stimulated genes (ISGs) in the PVR-transgenic mice. In the nontarget tissues, ISGs were expressed even in the noninfected state, and the expression level increased soon after poliovirus infection. On the contrary, in the target tissues, ISG expression was low in the noninfected state and sufficient response after poliovirus infection was not observed. The results suggest that the unequal IFN response is one of the important determinants for the differential susceptibility of tissues to poliovirus. We consider that poliovirus replication was observed in the nontarget tissues of PVR-transgenic/*Ifnar* knockout mice because the IFN response was null in all tissues.

The replication of many viruses is restricted to certain cells and tissues in the host. This tissue tropism results in a distinct disease pattern unique for each virus. Since virus infection initiates after binding of the virion to a receptor on the cell surface, cellular receptors for viruses have been considered the primary determinants of tissue tropism. However, following the identification of receptors for a number of viruses, it became apparent that receptor distribution in the host is wider than the virus replication sites (38). This indicates that virus tropism may be determined by another factor(s) in addition to the virus receptor.

Poliovirus, belonging to the genus *Picornaviridae*, is the causative agent of an acute human central nervous system disease, poliomyelitis (33). After poliovirus infection, the virus first multiplies in the oropharyngeal and intestinal mucosa and then in the lymphatic tissues, such as the tonsils and Peyer's patches. The virus drains into the blood and circulates within the body. Because visceral tissues, except for adipose tissues, seem to be nonpermissive for poliovirus infection, apparent pathological lesions are not observed in the nonneural tissues. Therefore, the site of virus multiplication during the viremic phase has not been identified. Finally, poliovirus reaches the central nervous system, which leads to the development of a paralytic disease in less than 1% of persons naturally infected with wild-type poliovirus (4, 23, 35). Even in the central nervous system, the poliovirus antigen, nerve cell changes, and inflammatory reactions are localized mainly in motor neurons in the anterior horn of the spinal cord and neurons in the brainstem. The brainstem as far as the hypothalamus and thalamus bears most of the cerebral pathological changes in poliomyelitis. The cerebral cortex (except for the motor cortex), basal ganglia (except occasionally for the globus pallidus), and the cerebellar cortex (except for the vermis) are rarely affected (2, 6). In terms of modern molecular biology, tissue tropism may be determined by interactions between host and viral factors. It is therefore important to elucidate the molecular mechanism responsible for tropism.

The poliovirus receptor (PVR) has been considered a major determinant of poliovirus tissue tropism (13). The molecular cloning of the human *PVR* gene was reported more than a decade ago (18, 24). With cultured cells, susceptibility of poliovirus infection completely correlates with the presence of functional PVR. However, in vivo, this rule is not always true. Analyses of PVR expression in humans revealed that there are many tissues, such as the liver and kidneys, that express PVR but are not involved in the infection (18, 24). Transgenic mice expressing the human *PVR* gene with its natural promoter (PVR-transgenic mice) were produced as a new animal model

* Corresponding author. Mailing address: Department of Microbiology & Immunology, Tokyo Metropolitan Institute for Neuroscience, Tokyo Metropolitan Organization for Medical Research, Musashidai, Fuchu-shi, Tokyo 183-8526, Japan. Phone: 81-42-325-3881. Fax: 81-42-321-8678. E-mail: koike@tmin.ac.jp.

for the study of poliovirus pathogenicity (21, 32). PVR-transgenic mice exhibited a paralytic disease that resembled human poliomyelitis after poliovirus infection. PVR mRNA was detected in all tissues of PVR-transgenic mice by Northern blot hybridization, although expression was restricted to certain cells, such as neurons in the central nervous system (20, 32) and Bowman's capsule and tubules in the kidney (32). PVR was also detected in the glomerulus in the kidney by immunofluorescent staining (15). These data suggest that PVR is necessary for poliovirus infection but may not be the sole determinant of tissue tropism (reviewed in reference 29). The results also suggest the existence of other factors that determine tissue tropism concomitantly with PVR expression. It is possible that host factors required for poliovirus replication are abundant only in target tissues or that host factors inhibiting virus replication are present in nontarget tissues.

To identify possible host factors, we produced another transgenic mouse strain in which there is ubiquitous PVR expression under the control of the CAG promoter (14). If we hypothesize that host factors required for poliovirus replication are present only in susceptible tissues, the distribution of poliovirus replication sites in the new transgenic mice would be the same as or wider than that in the transgenic mice previously produced, since the distribution of the PVR has broadened. However, after intracerebral infection, poliovirus propagated to a slight degree in neurons and glial and ependymal cells near the inoculation sites on day 1 postinfection (p.i.) but the virus titer decreased from day 2 p.i. without development of fatal encephalitis and poliomyelitis. After intraperitoneal and intravenous infection, no apparent signs of illness or virus replication were observed. It seemed to us that an unknown factor(s) that prevented virus replication and spreading was induced. This led us to hypothesize that an innate immune response, such as the production of interferon (IFN), may influence the pathogenesis of poliovirus.

Picornaviruses are sensitive to IFNs (7, 8, 25, 27, 49). IFN plays a central role in the innate immune antiviral response. Infected cells produce alpha/beta IFNs, which induce a number of genes, called IFN-stimulated genes (ISGs), that confer an antiviral state (36, 39, 41). In some viruses, including coxsackievirus and Theiler's virus, alpha/beta IFN plays an important role in the pathogenicity and tissue tropism of the virus (9, 10, 28, 34, 44). However, little is known about the role of alpha/beta IFNs in poliovirus pathogenesis.

Here we report the results of experiments that we conducted to assess the contribution of alpha/beta IFN in the pathogenesis of poliovirus infection with a PVR-transgenic mouse model (20, 21). PVR-transgenic mice were crossed with IFN-α/β receptor (IFNAR) knockout mice in which alpha/beta IFN signaling is disrupted (26). Poliovirus infection of the resulting PVR-transgenic/*Ifnar* knockout mice revealed that the IFN system is an important determinant of poliovirus tissue tropism and poliovirus pathogenesis.

MATERIALS AND METHODS

Cells, viruses, and mice. African green monkey kidney (AGMK) cell line JVK-03 (19) was maintained in Eagle's minimal essential medium supplemented with 5% fetal bovine serum. The poliovirus type 1 Mahoney strain was obtained by transfection of in vitro-synthesized RNA from infectious cDNA clone pOM (40) into JVK-03 cells. Virus titer was determined by a plaque assay on JVK-03 cells. A transgenic mouse strain, ICR-PVRtg21 (20, 21), was backcrossed for 10 generations with C57BL/6 mice, and then N10 mice were mated to obtain homozygotes (PVR-transgenic mice). The mouse strain deficient in the *Ifnar* gene, A129 (26), was purchased from B&K Universal Limited (United Kingdom) with the permission of M. Aguet. A129 was backcrossed for five generations with C57BL/6 mice and then with PVR-transgenic mice for two generations. $PVR^{+/+}$ $Ifnar^{-/-}$ mice were obtained by intercrossing these PVR-transgenic/*Ifnar* knockout mice.

Until the infection experiments, mice were maintained in an animal facility free of the following pathogens: *Citrobacter rodentium*, *Corynebacterium kutscheri*, *Mycoplasma pulmonis*, *Pasteurella pneumotropica*, *Salmonella* spp., cilia-associated respiratory bacillus, *Helicobacter hepaticus*, *Pseudomonas aeruginosa*, *Clostridium piliforme*, *Mycoplasma pulmonis*, ectromelia virus, lymphocytic choriomeningitis virus, mouse hepatitis virus, Sendai virus (HVJ), EDIM virus (rotavirus), minute virus of mice, mouse encephalomyelitis virus, pneumonia virus of mice, mouse adenovirus, reovirus type 3, ectoparasites, intestinal protozoa, and pinworm. Six-week-old mice were used for the experiments. All experiments with mice were performed in accordance with the Guidelines for the Care and Use of Laboratory Animals of the Tokyo Metropolitan Institute for Neuroscience.

Poliovirus infection in mice. Poliovirus at the indicated doses was inoculated intracerebrally, intravenously, or intraperitoneally as described previously (21). The mice were observed daily for 3 weeks or sacrificed at the indicated time p.i. The 50% lethal dose (LD_{50}) was calculated by the method of Kärber (45). In poly(I):poly(C) [poly(I:C)] protection experiments, 200 μg of poly(I:C) (Calbiochem) in phosphate-buffered saline was administered intracerebrally, and poliovirus challenge (10^4 PFU) was performed with the same inoculation routes on the next day.

Determination of virus titer in mouse tissues. Six mice inoculated with poliovirus were sacrificed on day 3 p.i. They were anesthetized and blood was collected from the heart. After perfusion with 20 ml of phosphate-buffered saline, the tissues were removed and frozen at −80°C. The tissues were thawed and homogenized in 5 to 10 ml of minimal essential medium. After centrifugation for 20 min at 3,000 × *g*, the virus titer of the supernatant was determined.

Histological and immunological examinations. Three to six mice were sacrificed on day 1, 2, or 3 p.i. or when the mice showed paralysis and were then used for histological examination. The mice were anesthetized and perfused with 10 ml of phosphate-buffered saline followed by 10 ml of 4% paraformaldehyde in phosphate-buffered saline. The fixed tissues were embedded in paraffin, from which 3-μm-thick sections were prepared. The poliovirus antigen was detected with an immunoperoxidase method as described previously (21).

Alanine aminotransferase and amylase activity. To evaluate the extent of liver injury in the mice, the serum alanine aminotransferase (ALT) level was measured with the Transnase Nissui kit (Nissui Pharmaceutical Co. Ltd.). The serum amylase level in the mice was measured by the method of Henkel et al. (12) with the Cica Auto amylase kit (Kanto Chemical Co. Inc.).

Quantitative real-time PCR. Mice tissues were separated immediately after sacrifice and stored at −80°C. Total RNA was isolated from the tissue with the RNeasy mini RNA isolation kit (Qiagen, Valencia, Calif.) according to the supplier's instructions. After DNase I treatment, cDNA primed with a random hexamer was synthesized with the Taqman reverse transcription reagent (Applied Biosystems, Foster City, Calif.). The quantification of RNAs was performed with ABI Prism 7900HT. 18S rRNA was quantified by the SYBR Green method with 18S-rRNA-F (5′-GTA ACC CGT TGA ACC CCA TT-3′) and 18S-rRNA-R (5′-CCA TCC AAT CGG TAG TAG CG-3′) as primers. Poliovirus RNA was quantified by the Taqman method with PV c-2493F (5′-TGG TTG GTG ACA GTT CTT ACA CAT T-3′) and PV c-2629R (5′-CCA CTG TGG CAC ACA GTG ATG-3′) as primers and PV c-2579T (5′-FAM-CCA TGT CGA ACG CAA AGC GCC-TAMRA-3′) as the probe. The detection of IFN-β, 2′-5′ oligoadenylate synthetase (OAS)1a, OAS1g, OAS2, OAS3, OASL2, protein kinase R, RIG-I, and helicard mRNAs was performed with Assay-on-Demand PCR probes (Applied Biosystems). The amount of mRNA was determined by comparison with standard templates of cloned cDNAs of known copy number. The expression levels were then normalized to the level of 18S rRNA.

RESULTS

Increased susceptibility of PVR-transgenic/*Ifnar* knockout mice to poliovirus. We previously produced transgenic mice expressing the human *PVR* gene (20, 21). *PVR* mRNA was detected in the brain, spinal cord, thymus, lungs, heart, stom-

TABLE 1. Susceptibility to poliovirus infection

Inoculation route	Mouse strain[a]	No. of mice dead/no. inoculated at inoculum dose (log_{10} PFU/mouse):										LD_{50} (log_{10})
		−1	0	1	2	3	4	5	6	7	8	
Intracerebral	PVR-tg	0/6	1/6	1/6	1/6	4/6	5/6	6/6				2.5
	PVR-tg/*Ifnar* KO	0/6	1/6	3/6	6/6	6/6						0.8
Intravenous	PVR-tg			0/6	1/6	1/6	4/6	3/6	6/6			5.0
	PVR-tg/*Ifnar* KO		0/6	0/6	5/6	6/6						1.7
Intraperitoneal	PVR-tg						0/6	1/6	3/6	5/6	5/6	>6.2
	PVR-tg/*Ifnar* KO		0/6	3/6	5/6	6/6						1.2

[a] tg, transgenic; KO, knockout.

ach, and muscle at high levels, in the spleen and kidneys at intermediate levels, and in the liver at low levels (data not shown). The PVR-transgenic mice were susceptible to poliovirus infection via the intracerebral, intraperitoneal, and intravenous routes. The infected mice developed a paralytic disease resembling human poliomyelitis. Unlike humans, however, PVR-transgenic mice were not highly susceptible to oral infection with poliovirus. We performed subsequent experiments with this transgenic mouse model.

Mice lacking the alpha/beta IFN response become highly susceptible to several virus infections (26). We compared the susceptibility of PVR-transgenic mice with that of PVR-transgenic/*Ifnar* knockout mice to poliovirus infection via intracerebral, intravenous, and intraperitoneal inoculations. The mice showed paralysis and died within 2 weeks p.i. in a dose-dependent manner following inoculation via all routes. This suggested that the mice died mainly due to poliovirus infection in the central nervous system irrespective of the inoculation route. The results and the LD_{50} values are shown in Table 1. The PVR-transgenic/*Ifnar* knockout mice were more sensitive to fatal poliovirus infection than the PVR-transgenic mice by any infection route. The LD_{50} value for PVR-transgenic/*Ifnar* knockout mice inoculated intracerebrally was 50-fold lower than that for PVR-transgenic mice. Notably, PVR-transgenic/*Ifnar* knockout mice became 3,000- and >20,000-fold more sensitive to poliovirus via intravenous and intraperitoneal inoculation, respectively. Furthermore, 10^6 PFU of poliovirus inoculated orally caused paralysis in 50% of the PVR-transgenic/*Ifnar* knockout mice (data not shown). On the contrary, PVR-transgenic mice with the disrupted IFN-γ gene (42) did not exhibit a significant increase in susceptibility to poliovirus infection (data not shown). The results indicate that alpha/beta IFN strongly influences poliovirus pathogenesis.

Distribution of poliovirus infection in PVR-transgenic/*Ifnar* knockout mice. Increased susceptibility to poliovirus by peripheral infection routes suggested that the poliovirus replicated efficiently in nonneural tissues. We compared poliovirus titers in the various tissues of nontransgenic C57BL/6 mice, PVR-transgenic mice, and PVR-transgenic/*Ifnar* knockout mice intravenously inoculated with 2×10^7 PFU of poliovirus. After intravenous inoculation, poliovirus was immediately delivered to all tissues, including the central nervous system, independently of the presence of PVR (47). Most of the PVR-transgenic mice and PVR-transgenic/*Ifnar* knockout mice developed paralysis by day 3 or 4 p.i., while the nontransgenic mice did not.

Figure 1 shows the virus load of various tissues on day 3 p.i. The virus titers in the brain and spinal cord of PVR-transgenic mice were much higher than those recovered from the same tissues of nontransgenic mice. The virus titer in the pancreas of PVR-transgenic mice was also higher than that of nontransgenic mice but not as high as the titers in the neural tissues of transgenic mice. The viral load of most of the other tissues of PVR-transgenic mice was slightly higher than that recovered from nontransgenic mice. These results suggest that poliovirus replicated efficiently in the central nervous system and less efficiently in the pancreas and did not replicate or replicated to only a slight degree in other nonneural tissues of PVR-transgenic mice. On the contrary, in PVR-transgenic/*Ifnar* knockout mice, poliovirus titers in all of the tissues examined were very high (Fig. 1), suggesting that the virus can replicate in nonneural tissues if alpha/beta IFN signaling is disrupted.

Poliovirus replication site in the visceral tissues of PVR-transgenic/*Ifnar* knockout mice. We investigated the localiza-

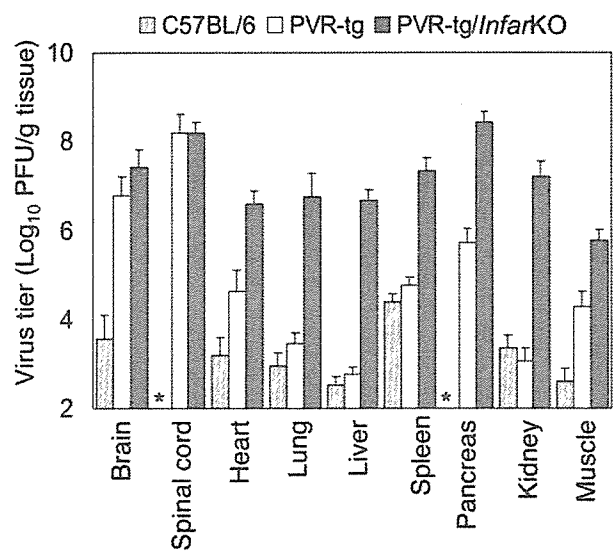

FIG. 1. Comparison of poliovirus titers in tissues of nontransgenic, PVR-transgenic, and PVR-transgenic/*Ifnar* knockout mice. The mice were inoculated intravenously with 2×10^7 PFU of poliovirus type 1 Mahoney strain. The tissues of nontransgenic mice (hatched bars), PVR-transgenic mice (open bars), and PVR-transgenic/*Ifnar* knockout mice (solid bars) were separated on day 3 p.i., and virus titers were determined by a plaque assay. The values represent the mean virus titer + standard deviation of six mice. The asterisk indicates that the values were below the limit of detection (2.0 log_{10} PFU/g).